# Scavenging of particulate and dissolved lead compounds by coprecipitation with manganese oxyhydroxides

Russell H. Abell

Submitted to the Faculty of the
Virginia Polytechnic Institute and State University
in partial fulfillment of the requirements of

MASTER OF SCIENCE

In

Geology

J. Donald Rimstidt, Chair
James R. Craig
Jodi J. Rosso

May 13, 1998
Blacksburg, Virginia

Keywords: manganese, lead, coprecipitation, borate, bicarbonate, quartz substrate, rates

**Scavenging of particulate and dissolved lead compounds by coprecipitation with manganese oxyhydroxides**

Russell H. Abell

(ABSTRACT)

Mn is a geochemically important element that contributes significantly to the cycling of heavy metals. During precipitation, Mn oxyhydroxides scavenge many heavy metals, including Pb, in a variety of natural environments. Because of this phenomenon, the precipitation of Mn oxyhydroxides may provide a remediation technique for removing Pb from contaminated aqueous solutions. Therefore, this study was undertaken to provide a quantitative understanding of the coprecipitation of Pb with Mn oxyhydroxides to demonstrate their capacity to remove Pb permanently from contaminated solutions. To accomplish this, a series of factorial experiments with varying initial Mn and Pb concentrations were run in the presence of a borate buffer or a bicarbonate buffer. All experiments were run in batch reactors, in the presence of a quartz substrate, at 25°C, at pH 8.5, and were continuously stirred. Initial Mn and Pb concentrations were varied by half log units from 100 to 0 mg/L and from 3 to 0 mg/L, respectively. Solutions were analyzed for Mn using the formaldioxime colorimetric method and for Pb using AA. Precipitates on quartz surfaces were analyzed by SEM, XPS, and XRD for precipitate identification and morphology. The amount of Mn and Pb associated with the quartz sand was determined by dissolving the precipitates from selected quartz samples using concentrated nitric acid. Finally, a different set of precipitate-coated quartz grains were leached in pH 5 acetic acid solution to assess the metal retention capacity of the precipitated material.

Mn oxyhydroxides precipitated onto the quartz sand in both the borate and bicarbonate buffered experiments. SEM and XPS data revealed tiny crystallites in etch pits on the quartz surfaces that contained predominantly $Mn^{3+}$. XRD analysis did not produce an X-ray pattern for these Mn oxyhydroxides but did identify the suspended Pb precipitates as hydrocerrusite and $PbB_2O_4$ in the borate buffered experiments and hydrocerrusite in the bicarbonate buffered experiments. Much more Mn and Pb are associated with the quartz surfaces in the borate buffered experiments, but no Pb was associated with quartz surfaces initially (< 6 hrs. of reaction time). Leaching of precipitates resulted in extracted Mn in both experiments but Pb was extracted in only the bicarbonate buffered experiments. The Mn precipitation rate was greater in the borate buffered experiments and higher initial Mn and Pb concentrations appear to increase the precipitation rate in both sets of experiments. These results indicate that Mn oxyhydroxides nucleated onto suspended Pb precipitates. The growing Mn oxyhydroxide particles were attracted to the quartz sand, carrying along the Pb precipitates. Further precipitation of Mn oxyhydroxides on the quartz surfaces trapped the Pb. This process was much more significant in the borate buffered experiments where much more Mn precipitated. The greater amount of Mn oxyhydroxide growth acts as a barrier protecting the Pb from the pH 5 leaching solutions. As a result, Pb was retained by the sand grains from the borate buffered experiments during leaching while significant amounts of Pb (35-100%) was extracted from the sand produced by the bicarbonate experiments. These results strongly suggest that coprecipitation of Pb with Mn

oxyhydroxides in the presence of a borate buffer and a quartz substrate may be a remediation tool for Pb contaminated aqueous solutions. Not only will this process remove aqueous $Pb^{2+}$ from solution but it appears it will also substantially incorporate colloidal Pb particles as well.

## ACKNOWLEDGEMENTS

At every way station in our lives there are many people who help us, guide us, and provide support while we accomplish the task at hand. Unfortunately, the recognition that these special people deserve is often elusive or confined to a page of text such as this. However, I hope that these people who have helped me through my career at Virginia Tech will remember my gratitude and appreciation for all of their guidance, efforts, and friendship.

First, I need to thank my advisor, Don Rimstidt, who has been there the whole way and provided a friendly and supportive environment for me to accomplish my research along with much guidance. I would also like to thank my committee, Jim Craig and Jodi Rosso for their support and helpful comments. Jodi has provided more help than could be imagined and I could not have finished without her wealth of knowledge and kindness. I would also like to thank the rest of the faculty for providing a great learning experience. And, I would like to thank all of the staff on the fourth floor: Mary, Connie, Linda, and Carolyn for always helping with the bureaucracy, being friendly, and listening to whatever I had to say. I would also like to thank all of my fellow graduate students, too many to mention all of them here. Eric thanks so much for all the help in the world on analytical geology and for listening to me blab on and on endlessly (as sometimes do). Thanks Maria, Amy (K.), Jay, Andrey, Luca, Jason, Jeane, Amy (J.), Jim, Rob, Peter and all of my past and current 4060 office mates for always being there to listen, drink beer, slack, and offer ideas/ advice. Thanks also goes to my roommate (and landlord) Ryan for always providing the non-Geo outlet and also for enduring endless complaints and questions. Thanks also goes to all my Vet school friends: Dan, Jen, Beth, and Allison (among others) for being there for fun times. I would like to thank all of my friends who do not reside in Blacksburg for their support and continued friendship, especially Julius who was always willing to go hiking or hang in DC when I needed some time away from the "Burg". Finally, I would like to thank my parents and brothers (Jon and Chris) for always believing in me and my abilities even at my lowest moments.

Finally, I would like to thank the organizations that provided financial support for this project. Funding was received from the Virginia Water Resources Research Center Mini-Grant, the Waste Policy Institute Summer Fellowship, and the Geological Society of America Penrose Grant.

Thanks to all you! And as I leave Blacksburg I will always carry my memories of you and our fun times with me.

## TABLE OF CONTENTS

## LIST OF TABLES

## LIST OF FIGURES

**Notation**

| | |
|---|---|
| $\{Mn\}_i$ = | concentration of Mn in solution at start of experiment (mg/L) |
| $\{Mn\}_t$ = | concentration of Mn in solution at time = t (mg/L) |
| $\{Pb\}_i$ = | concentration of Pb in solution at start of experiment (mg/L) |
| $\{Pb\}_t$ = | concentration of Pb in solution at time = t (mg/L) |
| $Q_{Mn}$ = | amount of Mn associated with quartz surfaces at 48 hours ($mg/m^2$) |
| $Q_{Pb}$ = | amount of Pb associated with quartz surfaces at 48 hours ($mg/m^2$) |
| $(Q_{Pb})_t$ = | amount of Mn associated with quartz surfaces at time = t ($mg/m^2$) |
| $E_{Mn}$ = | amount of Mn extracted from quartz surfaces at 48 hours ($mg/m^2$) |
| $E_{Pb}$ = | amount of Pb extracted from quartz surfaces at 48 hours ($mg/m^2$) |
| $m_i$ = | concentration of i (mol/kg) |

# CHAPTER 1: INTRODUCTION

Contamination of the environment by heavy metals continues to be a national concern. This concern results from the fact that heavy metals (e.g. As, Co, Cu, Ni, Pb, Zn) are toxic to soil microorganisms, plants, animals, and humans (Alloway, 1995 and references therein). These metals are typically released to the environment by mining wastes, industrial emissions, municipal wastes, and treated sewage, and so their concentrations are especially elevated in inhabited regions of the world (Nriagu and Pacyna, 1988). Although much research has focused on heavy metal mobility, behavior, pollution, and remediation in low-temperature geochemical settings, there are still many areas in which our understanding needs to be improved.

Manganese oxyhydroxides have been studied extensively because Mn is a geochemically important element and there is evidence that the geochemical cycling of many metals is strongly linked to Mn geochemistry. One of the potentially important processes controlling heavy metal behavior is the oxidation of $Mn^{2+}$ leading to precipitation as Mn oxyhydroxides. Many metals are closely associated with Mn oxyhydroxides in various natural settings (Jenne, 1968; Loganathan and Burau, 1973; Chao and Anderson, 1974; Crerar and Barnes, 1974; Carpenter et al., 1975; Dillard et al., 1982; Carpenter et al., 1978; Carpenter and Hayes, 1978; Robinson, 1981; Carlos et al., 1993; Lind and Hem, 1993). These settings include Mn coated stream boulders and sediments (Chao and Anderson, 1974; Carpenter et al., 1975; Carpenter et al., 1978), marine ferromanganese nodules (Loganathan and Burau, 1973; Crerar and Barnes, 1974; Dillard et al., 1982), and weathered fractures in high-silica igneous rocks (Carlos et al., 1993). These studies of Mn coated stream boulders, stream sediments, and ferromanganese nodules found that many different metals (e.g. Ag, Co, Cu, Ni, Pb, Zn) are associated with Mn oxide

coatings. Carpenter and Hayes (1978) and Robinson (1981) also found that Cu, Pb, and Zn can be coprecipitated with Fe-Mn oxides onto clean ceramic surfaces or sorbed onto Mn oxyhydroxide coatings directly from stream water containing anomalously high metal concentrations.

There are also several laboratory studies that identified precipitated Mn oxyhydroxides and studied Mn precipitation rates (Hem, 1963a, b; Coughlin and Matsui, 1976; Wilson, 1980; Hem, 1981; Sung and Morgan, 1981; Hem and Lind, 1983; Murray et al., 1985; Davies and Morgan, 1989; Junta and Hochella, 1994). Results from these studies indicate that initial Mn precipitates are typically $Mn^{3+}$ oxyhydroxides, such as hausmannite ($Mn_3O_4$), feitknecktite (β-MnOOH), and manganite (γ-MnOOH) (Hem, 1981; Hem and Lind, 1983; Murray et al., 1985; Junta and Hochella, 1994). Some of these studies found that during aging of the Mn precipitates, $Mn^{3+}$ oxidized further to form $Mn^{4+}$ oxides such as ramsdellite ($MnO_2$) and γ-$MnO_2$ (Hem and Lind, 1983; Hem and Lind, 1991).

Later investigations of Mn oxyhydroxide precipitation found that when $Mn^{2+}$ is oxidized in the presence of trace metals (e.g. Cu, Cd, Ni, Zn), a mixed Mn/trace metal oxyhydroxide forms by coprecipitation (Matsui, 1973; Hem, 1980; Hem et al., 1985; Hem et al., 1987; Hem at al., 1989; Hem and Lind, 1991). In two of these studies, a mixed Cu-Mn oxide ($Cu_2Mn_3O_8$) and Cd-Mn oxide ($Cd_2Mn_3O_8$) were identified by X-ray diffraction (Hem et al., 1989; Hem and Lind, 1991). These studies also document that initially a distinct heavy metal precipitate or colloid forms, followed by precipitation of $Mn^{3+}$ oxyhydroxides (Matsui, 1973; Hem et al., 1985; Hem et al., 1991). These heavy metal precipitates were colloidal Cu, Ni, and Zn hydroxides, CoOOH, and $CdCO_3$. Upon aging the $Mn^{3+}$ oxides disproportionate to $Mn^{4+}$ oxides and aqueous $Mn^{2+}$.

The resulting $Mn^{4+}$ precipitate incorporates the trace metal to form a mixed Mn/metal oxide, such as $Cu_2Mn_3O_8$ and $Cd_2Mn_3O_8$ (Hem et al., 1989; Hem and Lind, 1991). These investigators also found that the presence of trace metals (i.e. Co, Cu, Ni, Cd) in their systems increased the rate of Mn loss from solution (Matsui, 1973; Hem at al., 1989; Hem and Lind, 1991).

Mn precipitation in the presence of a substrate has also been investigated. Previous research documented that some mineral surfaces catalyze Mn oxidation and that Mn precipitates tend to nucleate and grow on the surfaces of minerals, such as clays, feldspars, hematite, lepidocrocite, goethite, and Mn-oxides (Hem, 1963a, b; Van der Weijden, 1975; Coughlin and Matsui, 1976; Wilson, 1980; Sung and Morgan, 1981; Davies and Morgan, 1989; Junta and Hochella, 1994). Van der Weijden (1975) showed that the Mn-oxides themselves have a stronger catalytic effect on Mn precipitation than the other substrates. These studies also found that the presence of the mineral surface enhances Mn precipitation rates.

In the laboratory studies summarized above, a wide range of anions were introduced into the systems to buffer the pH of the experiments or during addition of metal solutions. These anions include $H_3BO_3^o$, $SO_4^{2-}$, $NO_3^{2-}$, $HCO_3^-$, and $OH^-$. Most of these studies did not focus on how these various anions influence Mn precipitation and rates. However, a few earlier studies have documented differences due to the presence of $SO_4^{2-}$and $HCO_3^-$. Morgan (1967) and Hem (1963a) found that the presence of $SO_4^{2-}$ inhibited Mn precipitation rates. Hem (1963a) also found that $HCO_3^-$ retards the Mn precipitation rate. The presence of $SO_4^{2-}$ also caused different Mn oxyhydroxides to precipitate, $\gamma$-MnOOH and $\alpha$-MnOOH instead of $\beta$-MnOOH (Hem and Lind, 1983). These studies suggest that anions influence Mn precipitation mechanisms and the rate of precipitation.

Although much research has focused on the scavenging of metals by Mn oxyhydroxides, investigating the scavenging of Pb in the presence of a quartz substrate has not been investigated. In addition, much of the previous research has not focused on the effect of different anions on Mn precipitation and how the presence of anions might change the precipitation rate and precipitation mechanism. Because $H_3BO_3^o$ and $HCO_3^-$ contribute to the buffer capacity of many natural waters and mineral substrates are ubiquitous in these systems, it is important to understand their combined effect on the scavenging of metals by coprecipitation with Mn oxyhydroxides.

This study was undertaken to provide a quantitative understanding of the scavenging of Pb by coprecipitation with Mn oxyhydroxides. It compares the effect of $H_3BO_3^o$ and $HCO_3^-$ on the Mn precipitation rate and amount of Mn and Pb precipitated on quartz surfaces. By investigating these phenomenon, it was possible to characterize Pb and Mn coprecipitation in the presence of quartz and to determine the capability of the precipitated Mn oxyhydroxides to retain Pb. It was also possible to determine the influence of borate on Mn precipitation and precipitation rates. Finally, this study demonstrated that coprecipitation of Mn with Pb onto mineral surfaces is a potentially cost-effective remediation tool for Pb contaminated aqueous systems.

# CHAPTER 2: METHODS

*Batch reactor experiments*

A series of factorial experiments were performed in batch reactors where the initial $Mn^{2+}$ concentration, $\{Mn\}_i$, and the initial $Pb^{2+}$ concentration, $\{Pb\}_i$, were varied systematically while the pH was held constant at 8.5. In the experiments, $\{Mn\}_i$ ranged from 100 mg/L to 0 mg/L by half log units and $\{Pb\}_i$ ranged from 3 to 0 mg/L. All experiments were run in triplicate. In each series of experiments, except $\{Pb\}_i = 0$ mg/L experiment, one sample contained $\{Mn\}_i = 0$ mg/L for control. The substrate for Mn precipitation in all of these experiments was HCl-washed quartz grains. Four additional experiments containing no quartz substrate were run for control of the entire procedure. Finally, one set of experiments was run at constant $\{Mn\}_i$ and $\{Pb\}_i$ and sampled at specific time intervals to measure the rate of Mn precipitation.

The pH of these experiments was held constant at 8.5 using either a boric acid ($H_3BO_3$)-sodium hydroxide (NaOH) buffer, or a sodium bicarbonate ($NaHCO_3$)-sodium carbonate ($Na_2CO_3$) buffer. The borate buffer contained 0.01 *m* $H_3BO_3$ and the bicarbonate buffer contained 0.01 *m* $NaHCO_3$ and $1.65 \times 10^{-3}$ *m* $Na_2CO_3$. Previous Mn oxidation studies have used both borate and bicarbonate buffers (Wilson, 1980; Sung and Morgan, 1981; Davies and Morgan, 1989). The following reagents were combined with the buffers to make the experimental solutions: $1.8 \times 10^{-2}$ *m* $MnCl_2$, $4.0 \times 10^{-4}$ *m* $MnCl_2$, and $6.0 \times 10^{-5}$ *m* $Pb(NO_3)_2$. After adding the above reagents, the batch reactors were placed in a shaker bath at ~175 or ~65 excursions/ minute for 48 hours. All experiments were carried out in triplicate and the mean values +/- 1 standard deviation are given in the Results section. Visual observations and pH were recorded at 3 hours, 6 hours, 12 hours, 24 hours, 36 hours, and 48 hours. At the end of each experiment 30 mL of

solution was extracted for $\{Pb\}_{48hr}$ and $\{Mn\}_{48hr}$ analysis and the final pH was measured. The remainder of the solution was discarded and the quartz grains were rinsed in distilled, de-ionized (D.D.I.) water three times. The grains were then dried at 60°C for 0.5 hour before being stored for SEM and XPS analysis. For detailed experimental procedures, refer to Appendix 1.

*Substrate*

The quartz grains used in these experiments ranged in size from 0.42 mm to 1.0 mm, however, more than 85% were < 0.84 mm. The grains are well-rounded and well-sorted. The surface area of the grains, after the grains were washed in an HCl solution, was determined to be 0.11 $m^2\ g^{-1}$ from BET surface area analysis. These HCl-washed grains were analyzed by SEM to identify surface features and impurities. The surfaces of most of the quartz grains displayed abundant etch pits and larger pitted or abraded areas. EDS analysis showed Al and K peaks and these peaks may be attributed to small amounts of fine-grained clay on the quartz surfaces. The grains were prepared for experiments by soaking in 100 mL of 1.2 *m* HCl for 1 hour. The grains were then rinsed with distilled, de-ionized water until the supernatant pH was greater than five. Finally, the grains were dried at 60°F and 3 g of quartz was allocated for each experiment.

*Analytical techniques and sample analysis*

The concentration of Mn and Pb in solution at the end of the experiments ($\{Mn\}_{48hr}$ and $\{Pb\}_{48hr}$, respectively) and the final pH of the solutions were all measured for each experiment. The pH was measured using a FisherScientific® Accumet 10 pH meter. $Mn^{2+}$ concentrations were determined using the formaldioxime colorimetric method of Morgan and Stumm (1965). A Milton-Roy® Spectronic 21D spectrophotometer was used to measure the absorbance of each solution. The spectrophotometer uses a 1 cm cell. The detection limit for this procedure is 0.35

mg/L. A series of standards were analyzed to produce a calibration curve of absorbance versus concentration and the concentration of subsequent unknowns was determined using this calibration curve. A detailed procedure of this analysis and the calibration curve is presented in Appendix 1. Analysis of $Pb^{2+}$ in solution was performed using a Buck Scientific 200-A atomic absorption spectrophotometer (AA). A series of standards were analyzed to produce a calibration curve of absorbance versus concentration and the concentration of subsequent unknowns was determined using this calibration curve. The detection limit for this analysis is 0.2 mg/L. A detailed procedure and calibration curves for Pb analysis are presented in Appendix 1. Finally, samples of experimental solutions were not filtered before Mn and Pb analysis unless suspended Mn precipitates were observed.

Some Mn-coated quartz grains were digested in concentrated nitric acid to dissolve all precipitates. The grains were soaked in a 50 mL solution containing 10-25 mL of nitric acid until the quartz sand no longer contained precipitates. The resulting solution was diluted to 200 mL and analyzed for $Mn^{2+}$ and $Pb^{2+}$ concentrations as described above. A detailed description of the digestion process is available in Appendix 1.

Reacted quartz grains and suspended precipitates were also analyzed by a Cambridge Instruments Camscan 2 scanning electron microscope (SEM), a Scintag 2000 X-ray diffractometer (XRD), and PHI electronics X-ray photoelectron spectroscopy (XPS). Sample preparation for the SEM involved mounting quartz grains in epoxy. Quartz grains were attached to aluminum mounts with double-sided sticky tape for XPS and XRD analysis. Sample preparation for XRD also included suspended precipitates recovered by filtering the solutions through 1.0 μm filters (cellulose nitrate membrane) and then attaching the filters to one inch glass

slides. The magnitude of the multiplet splitting of the Mn3s peaks from the XPS data was used to determine the Mn oxidation states on the quartz surfaces. This method has been used by Junta and Hochella (1994) and others. The distance between the two split Mn3s peaks is different for each oxidation state of Mn. Therefore, by analyzing these magnitudes, Mn oxidation states can be determined. Relative Mn/Si and Pb/Si peak area ratios on the quartz surfaces were also determined from the XPS data. Peak areas were normalized by dividing the peak areas by their cross-sectional areas reported in Yeh and Lindau (1985) before calculating the ratios.

Finally, Mn-coated quartz grains were leached in a pH 5 acetic acid (HAc)- sodium hydroxide (NaOH) buffered solution to determine how stable the precipitates might be in mildly acidic solutions containing organic ligands that can complex the metals. The quartz sand was soaked in 75 mL of the pH 5 buffer for 5 hours. The resulting solution was diluted to 200 mL and analyzed for $Mn^{2+}$ and $Pb^{2+}$ concentrations as described above. For a detailed procedure of the leaching process refer to Appendix 1.

# CHAPTER 3: RESULTS

Quartz sand from the borate buffered experiments and the bicarbonate buffered experiments are shown in Figures 1a and 1b, respectively. These figures show that precipitate has grown on the quartz grains and that the surface coatings of brown precipitate decrease in color intensity with decreasing $\{Mn\}_i$ and $\{Pb\}_i$. These figures also qualitatively demonstrate the amount of Mn precipitated increases as $\{Mn\}_i$ increases, as $\{Pb\}_i$ increases, and in the presence of the borate buffer. Precipitated Mn oxyhydroxides also coated the walls of the glass flasks in all experiments and suspended precipitates were observed after 24 hours in the borate buffered experiments with highest $\{Mn\}_i$. No attempt was made to quantify the amount of Mn precipitated on the flask walls or as suspended precipitates. However, these suspended brown Mn precipitates were observed in the borate buffered experiments after at least 24 hours of reaction time when Pb was present. The suspended precipitates were only observed in runs with $\{Mn\}_i > 10$ mg/L. No similar observations for the bicarbonate experiments were recorded.

*Nature of precipitated material*

SEM investigations showed that Mn oxyhydroxides covered a majority of the surface. Tiny crystallites were observed in etch pits and abraded areas that were not in contact with other surfaces during the reaction (see Figure 2). In addition, EDS analysis of the quartz surfaces produced Mn peaks and weak Pb peaks.

Selected samples were also analyzed using XPS. Mn/ Si and Pb/ Si ratios were calculated from these data and are in Table 1. Pb/ Mn ratios can then be calculated from the metal/ Si ratios and are 0.03 for borate buffered experiments and 0.27 for bicarbonate buffered experiments. Mn oxidation states of the precipitates on quartz surfaces were determined from XPS spectra of

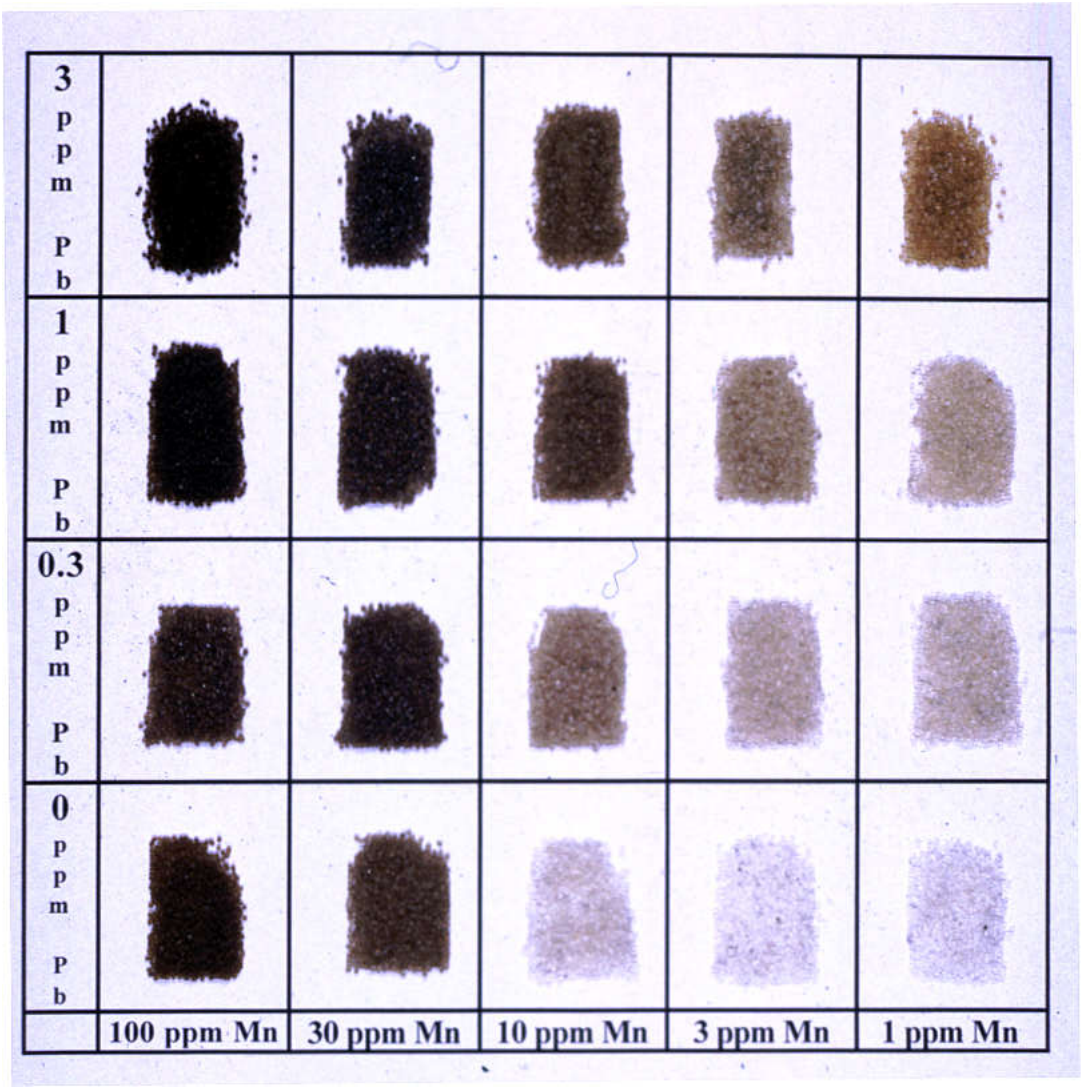


Figure 1a: Mn-coated quartz sand grains from borate buffered experiments. Color intensity reflects the amount of Mn precipitated on the surface. Each row represents different initial concentrations of Pb ($\{Pb\}_i$) and each column represents different initial concentrations of Mn ($\{Mn\}_i$). Reaction time was 48 hours for all grains.

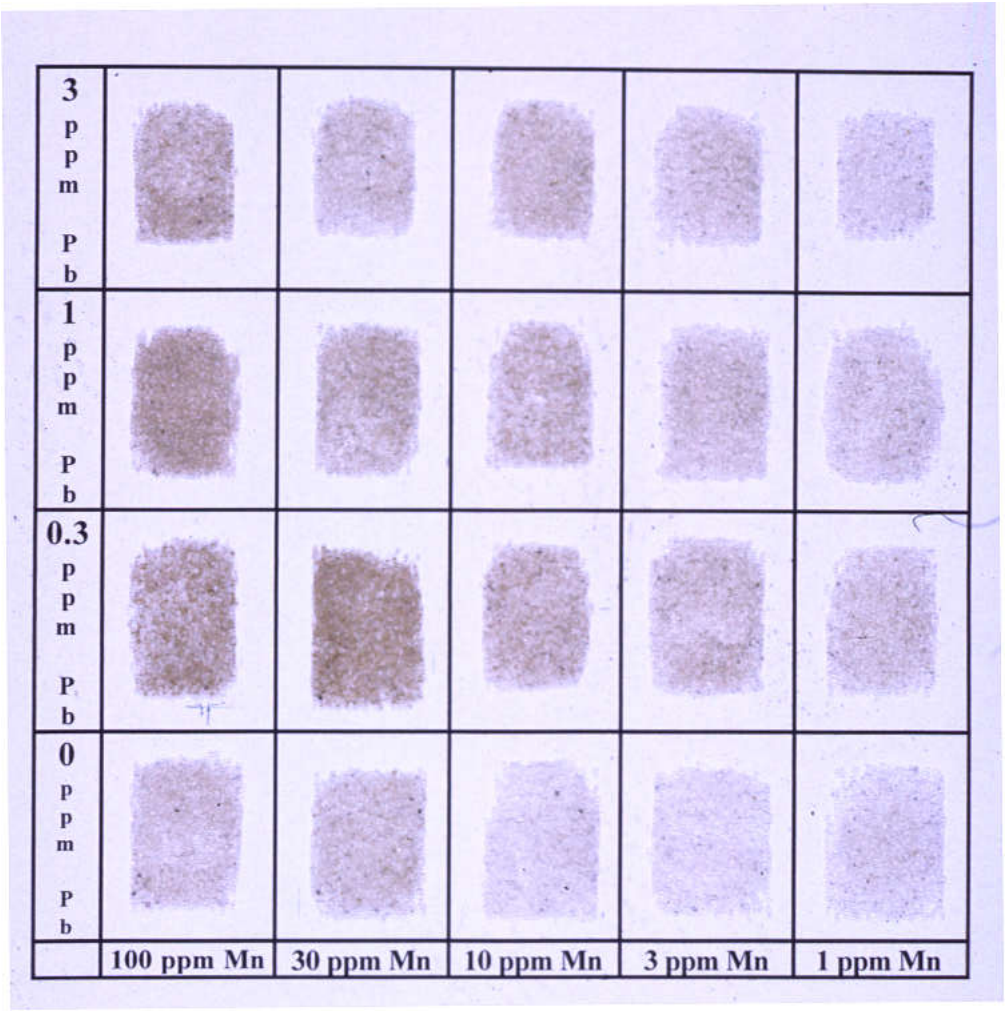


Figure 1b: Mn-coated quartz sand grains from bicarbonate buffered experiments. Color intensity reflects the amount of Mn precipitated on the surface. Each row represents different initial concentrations of Pb ($\{Pb\}_i$) and each column represents different initial concentrations of Mn ($\{Mn\}_i$). Reaction time was 48 hours for all grains.

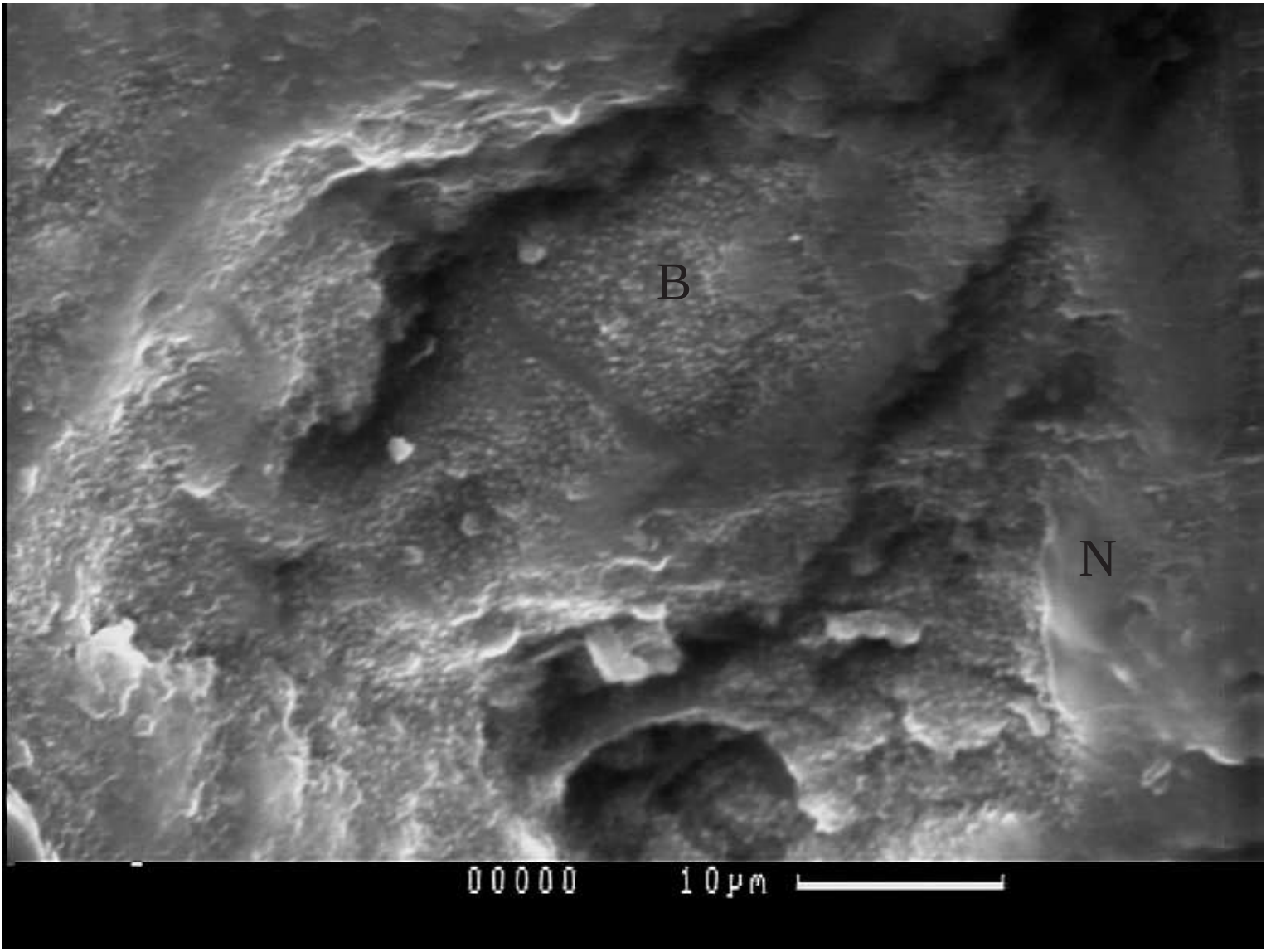


Figure 2: SEM image (SEI) of a quartz grain surface showing pitted regions covered with Mn oxyhydroxide crystallites (B) and terrace regions that do not contain visible crystallites (N) due to abrasion. Scale bar is 10 microns. Sample reacted for 48 hours in the borate buffer with $\{Mn\}_i$ = 100 mg/L and $\{Pb\}_i$ = 3 mg/L. These crystallites were observed on numerous quartz grains from this experiment.

Table 1: Mn/Si, Pb/Si, and Pb/Mn ratios of XPS data from quartz surfaces. Sample brB7rha-2 was run with $\{Pb\}_i$ = 3 mg/L and for 60 days. Samples brB8rha-1, brB8rha-6, brD5rha-1, and brD5rha-6 were run with $\{Pb\}_i$ = 3 mg/L and for 48 hours.

| Sample ID | Sample Description | Mn/ Si | Pb/ Si (x 10) |
|---|---|---|---|
| brB7rha-2 | $\{Mn\}_i$ = 100 ppm, borate experiments | 3.18 | 0.95 |
| brB8rha-1 | $\{Mn\}_i$ = 100 ppm, borate experiments | 1.66 | 0.50 |
| brB8rha-6 | $\{Mn\}_i$ = 0 ppm, borate experiments | | 0.45 |
| brD5rha-1 | $\{Mn\}_i$ = 100 ppm, bicarbonate experiments | 0.13 | 0.35 |
| brD5rha-6 | $\{Mn\}_i$ = 0 ppm, bicarbonate experiments | | 0.27 |

Mn3s peaks. The Mn3s peaks were fit using the technique described by Junta and Hochella (1994) and these fits are presented in Figure 3. The fitted spectra show that $Mn^{3+}$ is the dominant Mn species on the surface of quartz sand from the borate buffered experiment after 48 hours of reaction time. After 60 days of reaction time, the Mn oxyhydroxides clearly consist of a mixture of $Mn^{3+}$ and $Mn^{4+}$. The intensities of the Mn3s peaks from Mn oxyhydroxides grown in the bicarbonate system were too low for analysis of Mn oxidation states. XPS survey spectra are available in Appendix 2 (Figures C1.1-C1.5). Precipitate-coated quartz grains from both sets of experiments were also analyzed using XRD but no patterns were observed for Mn oxyhydroxide precipitates.

Pb solution data were similar for the borate and bicarbonate buffered experiments. $\{Pb\}_{48hr}$ was below detection (0.2 mg/L) in all experiments. In addition, rate experiments showed that $\{Pb\}_{3hr}$ was also below detection. Upon addition of the $Pb(NO_3)_2$ reagent, a white precipitate was observed to form in the borate buffered experiments and this precipitate emanated from where the Pb reagent made initial contact with the buffer solution. In the bicarbonate buffered experiments, no white precipitate was observed but the solution turned cloudy white soon after the Pb reagent was added. XRD was used to identify the Pb-precipitate formed upon initial addition of reagent to the buffers. These results showed that Pb-borate [$PbB_2O_4 \bullet H_2O$] and hydrocerrusite [$Pb_3(CO_3)_2(OH)_2$] formed in the borate buffered experiments but only hydrocerrusite formed in the bicarbonate buffered experiments. The XRD patterns are presented in Appendix 2 (Figures B1.1-B1.2).

Table 2 lists the data from the digestion of quartz grains prepared in experiments with $\{Pb\}_i$ = 3 mg/L to determine the amount of Mn ($Q_{Mn}$) and the amount of Pb ($Q_{Pb}$) associated with

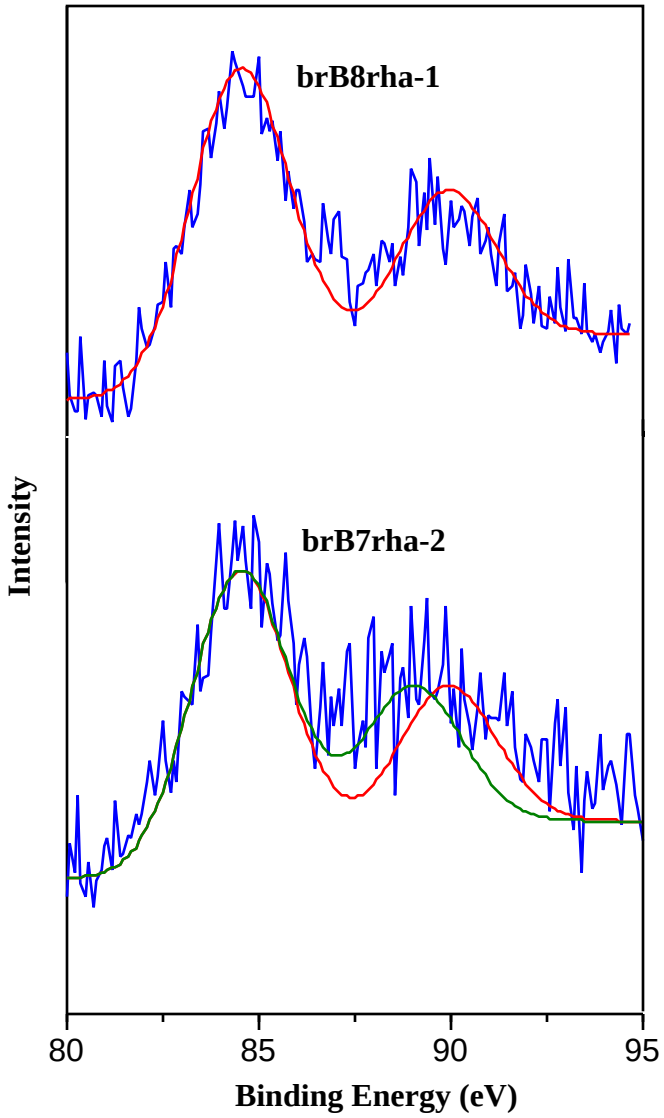


Figure 3: XPS spectra of Mn3s peaks and oxidation state curve fits for the Mn3s peak split. $Mn^{3+}$ is represented by the red curve fit and $Mn^{4+}$ by the green curve fit. Both samples contained $\{Mn\}_i$ = 100 mg/L and $\{Pb\}_i$ = 3 mg/L and are from the borate buffered experiments. However, the reaction time was 60 days for sample brB7rha-2 and 48 hours for sample brB8rha-1.

Table 2: Amount of Mn and Pb associated with quartz surfaces for borate and bicarbonate buffered experiments (1 standard deviation of the mean is given in parentheses). This digestion procedure was performed on $\{Pb\}_i$ = 3 mg/L experiments only.

**A) Mn associated with quartz surfaces:**

| $\{Mn\}_i$ (mg/L) | $Q_{Mn}$ Borate buffered experiments (mg/m$^2$) | $Q_{Mn}$ Bicarbonate buffered experiments (mg/m$^2$) |
|---|---|---|
| 100 | 5.41 (0.66) | 1.44 (0.23) |
| 30 | 3.41 (0.34) | 0.98 (0.20) |
| 10 | 1.20 (0.20) | 0.68 (0.10) |
| 3 | 1.04 (0.26) | 0.69 (0.19) |
| 1 | 0.28 (0.04) | 0.43 (0.07) |

**B) Pb associated with quartz surfaces:**

| $\{Mn\}_i$ (mg/L) | $Q_{Pb}$ Borate buffered experiments (mg/m$^2$) | $Q_{Pb}$ Bicarbonate buffered experiments (mg/m$^2$) |
|---|---|---|
| 100 | 0.48 (0.07) | 0.25 (0.05) |
| 30 | 0.49 (0.05) | 0.32 (0.05) |
| 10 | 0.55 (0.10) | 0.53 (0.15) |
| 3 | 0.58 (0.05) | 0.41 (0.13) |
| 1 | 0.37 (0.02) | 0.25 (0.05) |
| 0 | 0.27 (0.01) | 0.22 (0.04) |

**C) Pb/Mn ratios on quartz surfaces:**

| $\{Mn\}_i$ (mg/L) | $Q_{Pb}/Q_{Mn}$ Borate buffered experiments | $Q_{Pb}/Q_{Mn}$ Bicarbonate buffered experiments |
|---|---|---|
| 100 | 0.09 | 0.18 |
| 30 | 0.14 | 0.32 |
| 10 | 0.45 | 0.77 |
| 3 | 0.56 | 0.60 |
| 1 | 1.30 | 0.59 |

the quartz (see Table 2). A complete listing of these data is available in Appendix 3 (Table D). Figures 4 and 5 show how $Q_{Mn}$ and $Q_{Pb}$ vary as $\{Mn\}_i$ increases. $Q_{Pb}$ / $Q_{Mn}$ ratios versus $\{Mn\}_i$ are presented in Figure 6. Finally, quartz grains in $\{Pb\}_i$ = 3 mg/L rate experiments were digested in nitric acid to determine how $Q_{Pb}$ varied with reaction time and these data are presented in Figure 7. These data are also available in Appendix 3 (Table G).

In addition to the nitric acid digestion procedure, selected, precipitate-coated quartz grains were leached in a pH 5 acetic acid solution for five hours. Values for the amount of Mn and Pb extracted ($E_{Mn}$ and $E_{Pb}$, respectively) are presented in Table 3. A complete list of the data is available in Appendix 3 (Table E). Figure 8 shows how the $Q_{Pb}$ / $Q_{Mn}$ ratio changes as this leaching process proceeds for the borate and bicarbonate buffered experiments. Figure 9 shows how $E_{Mn}$ varies as a function of $\{Mn\}_i$ for the borate and bicarbonate buffered experiments.

*Mn precipitation rate*

The relative amounts of Mn precipitated at the end of experiments ($\{Mn\}_i$ - $\{Mn\}_{48hr}$) for the borate and bicarbonate buffered experiments are compared in Figures 10a and 10b. The most significant result shown by Figure 10 is that more Mn was precipitated in the borate buffered experiments. Figure 10 also shows that $\{Mn\}_i$ and $\{Pb\}_i$ influenced the amount of Mn precipitated. For each experiment $\{Mn\}_i$ - $\{Mn\}_{48hr}$ data are presented in Table 4 with an associated standard deviation. A complete listing of all experimental data is in Appendix 3 (Tables A and B).

A set of experiments using both borate and bicarbonate buffers was run with $\{Mn\}_i$ = 10 mg/L and $\{Pb\}_i$ = 3 mg/L to determine $\{Mn\}_t$ (see Figure 11). The solution data for these experiments are available in Appendix 3 (Table C). A polynomial fit of the form $a + bt + ct^2$ was

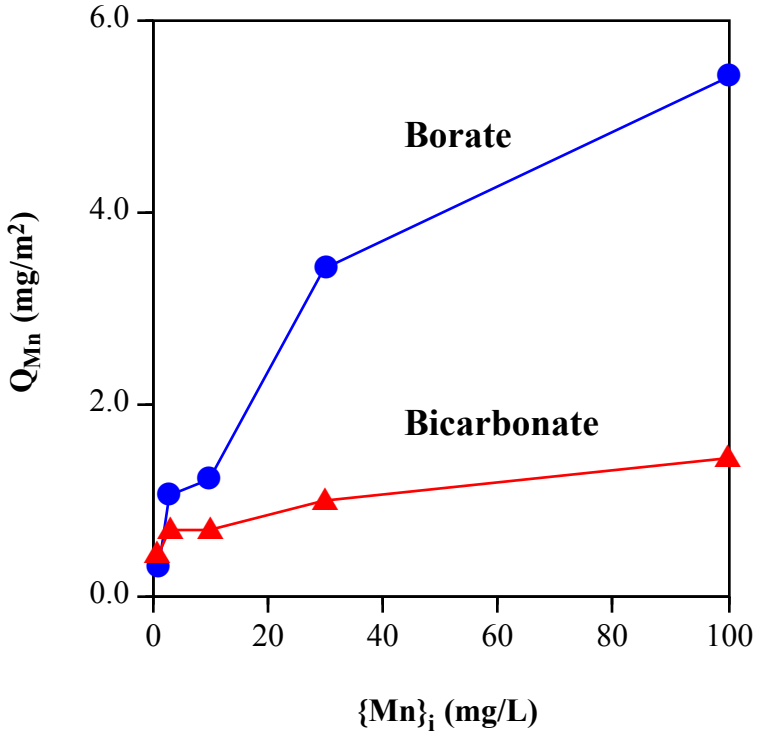


Figure 4: Amount of Mn associated with quartz surfaces after 48 hours as a function of $\{Mn\}_i$ in the experiments. Data are from experiments with $\{Pb\}_i$ = 3 mg/L.

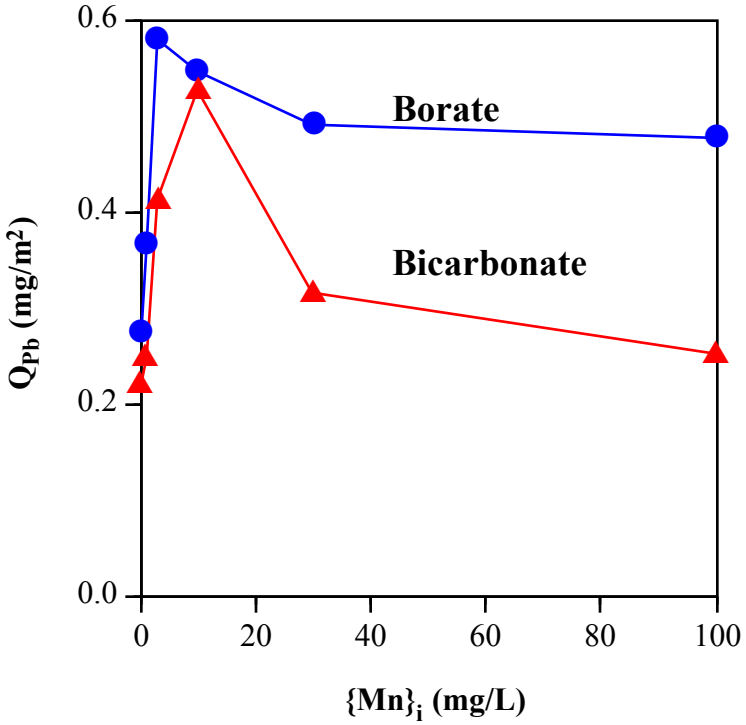


Figure 5: Amount of Pb associated with quartz surfaces after 48 hours as a function of $\{Mn\}_i$ in the experiments. Data are from experiments with $\{Pb\}_i$ = 3 mg/L .

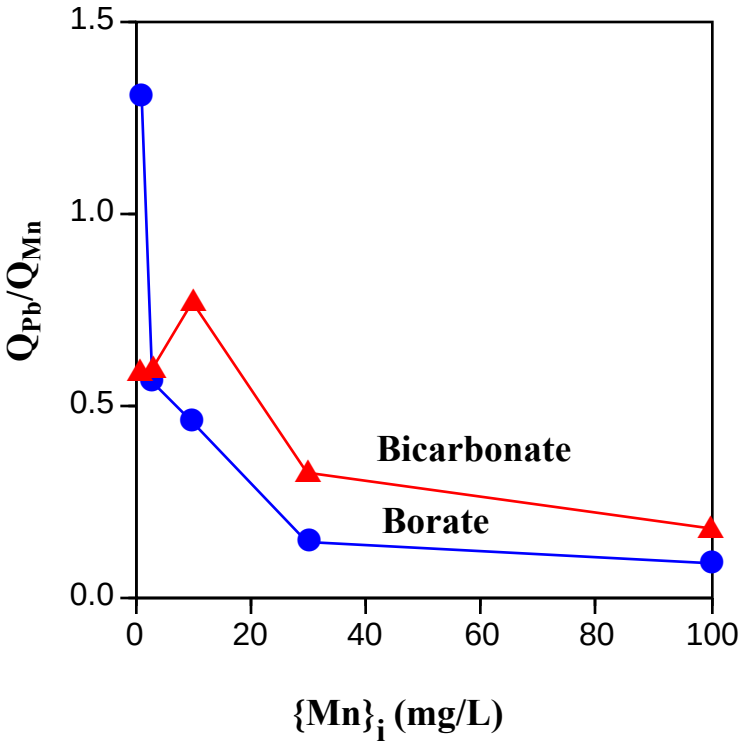


Figure 6: Pb/Mn ratio on quartz surfaces after 48 hours as a function of initial Mn concentration. Data are from experiments with $\{Pb\}_i$ = 3 mg/L.

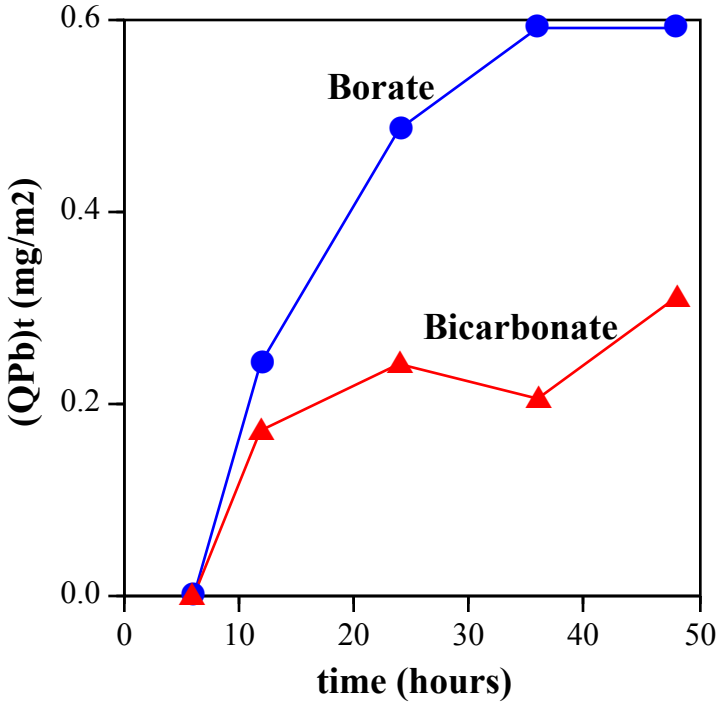


Figure 7: Amount of Pb associated with quartz surfaces as a function of time. Data are from experiments with $\{Mn\}_i$ = 10 mg/L and $\{Pb\}_i$ = 3 mg/L.

Table 3: Amount of Mn and Pb extracted from quartz surfaces by a pH 5 acetic acid leach procedure (1 standard deviation from the mean are given in parentheses). This procedure was performed on $\{Pb\}_i$ = 3 mg/L experiments only.

**A) Amount of Mn extracted from quartz surfaces**

| $\{Mn\}_i$ (mg/L) | Borate buffered experiments: ($mg/m^2$) | (%) | Bicarbonate buffered experiments: ($mg/m^2$) | (%) |
|---|---|---|---|---|
| 100 | 1.84 (0.77) | 34 | 1.10 (0.64) | 77 |
| 30 | 1.26 (0.49) | 37 | 0.45 (0.19) | 46 |
| 10 | 0.31 (0.19) | 26 | <0.21 | <31 |
| 3 | <0.21 | <21 | 0.40 (0.44) | 57 |
| 1 | <0.21 | <76 | <0.21 | <50 |

**B) Amount of Pb extracted from quartz surfaces**

| $\{Mn\}_i$ (mg/L) | Borate buffered experiments: ($mg/m^2$) | (%) | Bicarbonate buffered experiments: ($mg/m^2$) | (%) |
|---|---|---|---|---|
| 100 | <0.12 | <25 | 0.22 (0.02) | 88 |
| 30 | <0.12 | <25 | 0.17 (0.03) | 54 |
| 10 | <0.12 | <22 | 0.24 (0.04) | 46 |
| 3 | <0.12 | <21 | 0.15 (0.02) | 37 |
| 1 | <0.12 | <33 | 0.17 (0.00) | 68 |
| 0 | <0.12 | <44 | 0.22 (0.12) | 100 |

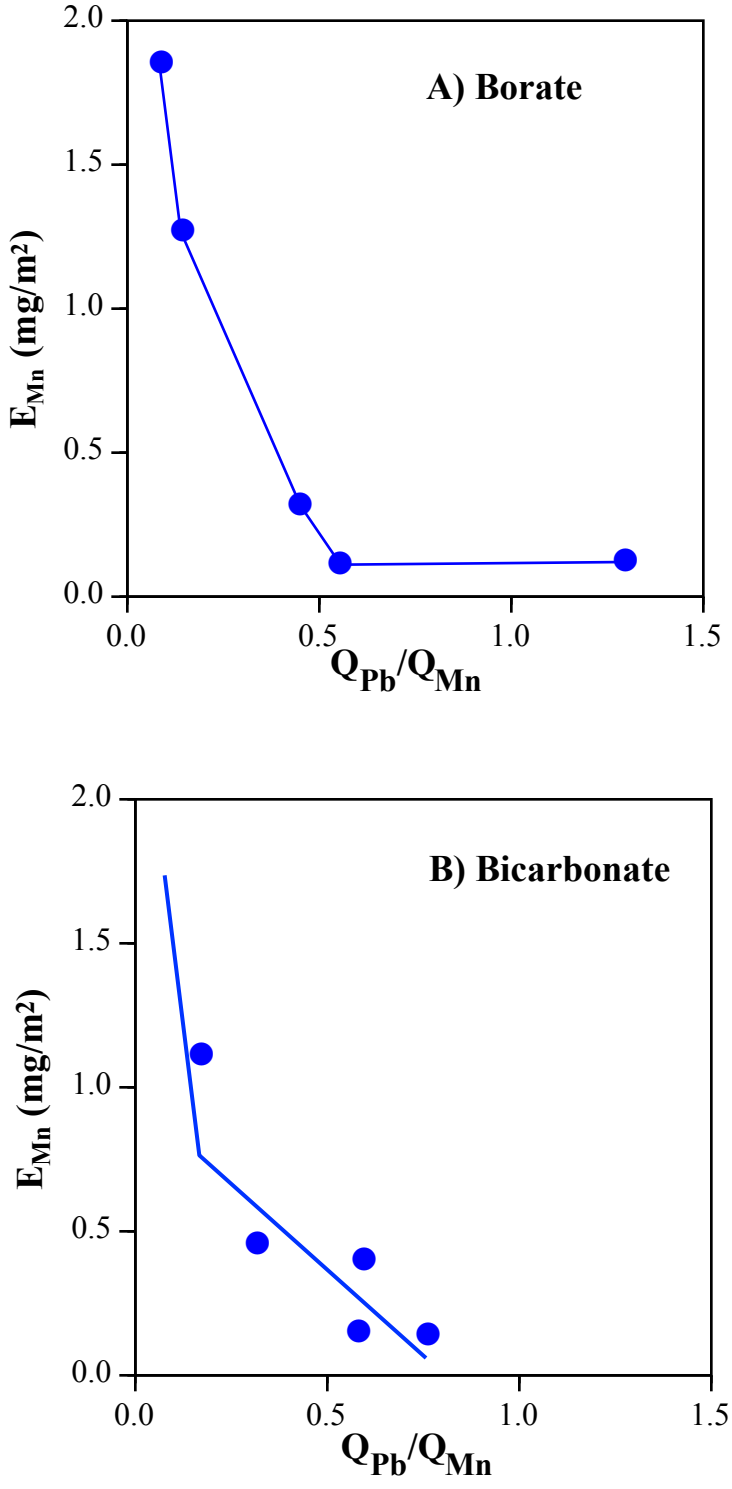


Figure 8: Amount of Mn extracted from quartz surfaces by an acetic acid leach as a function of the Pb/Mn ratio on the surface. Data are from experiments with $\{Pb\}_i$ = 3 mg/L after 48 hours. A) Borate buffered experiments. B) Bicarbonate buffered experiments.

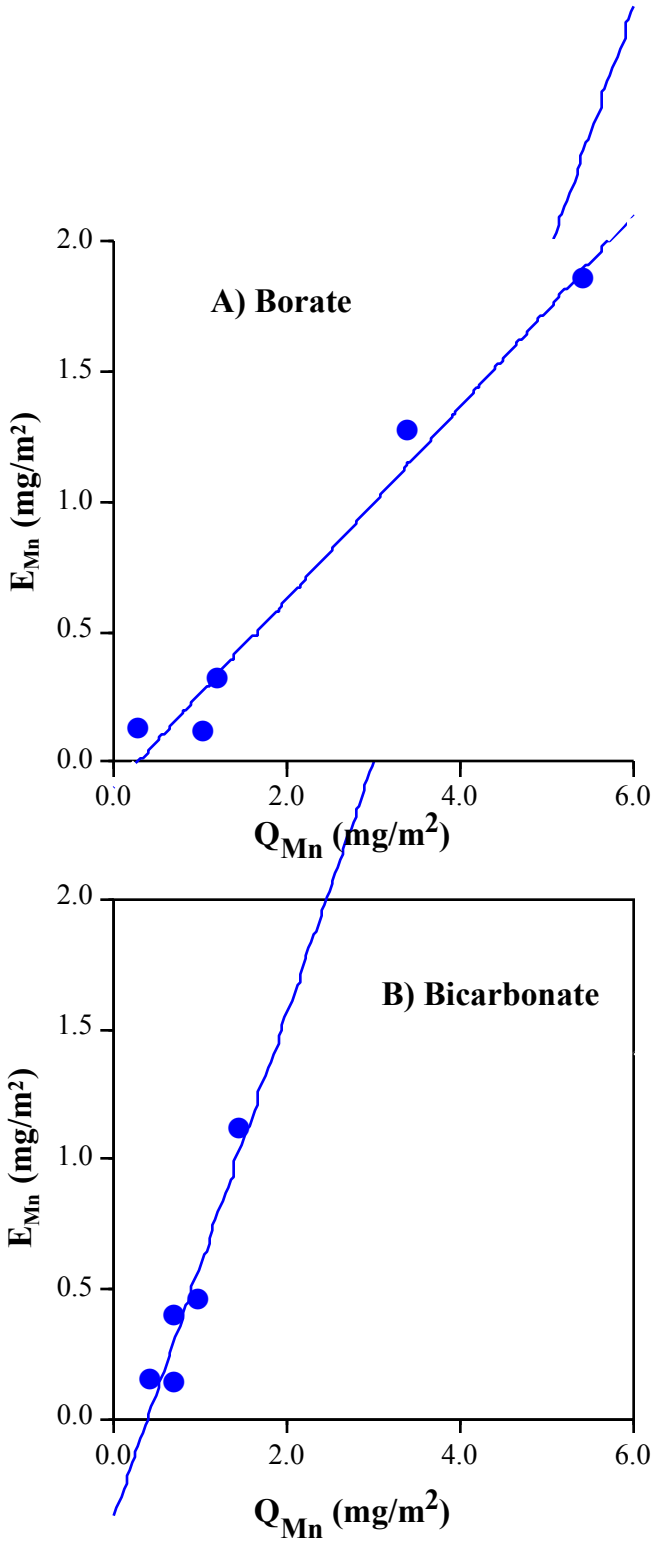


Figure 9: Amount of Mn extracted from quartz surface as a function of the amount of Mn associated with quartz surfaces. Data are from acetic acid leaching of Mn-coated quartz sand prepared in experiments with $\{Pb\}_i$ = 3 mg/L after 48 hours. A) borate buffered experiments. B) bicarbonate buffered experiments.

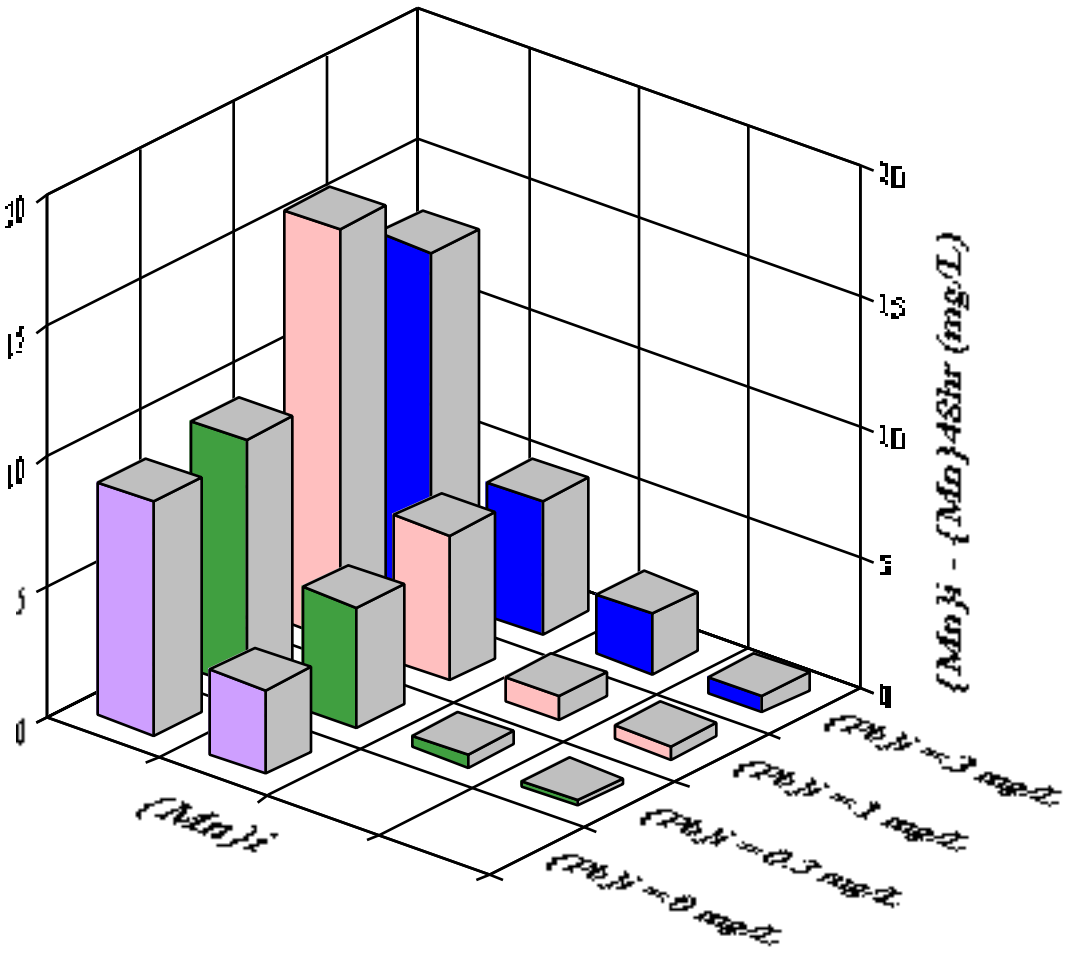


Figure 10a: Amount of Mn precipitated, $\{Mn\}_i$ - $\{Mn\}_{48hr}$, as a funtion of $\{Mn\}_i$ and $\{Pb\}_i$ in the borate buffered experiments after 48 hours.

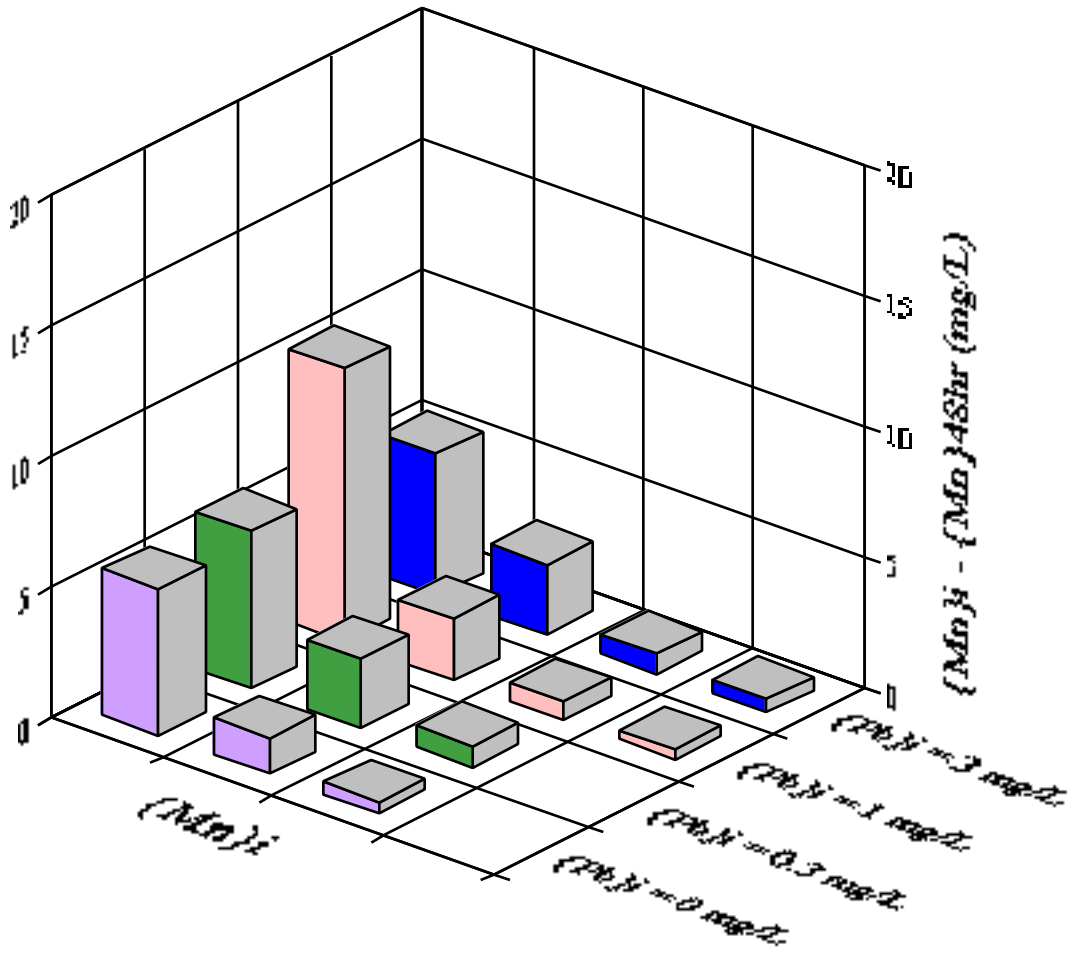


Figure 10b: Amount of Mn precipitated, $\{Mn\}_i$ - $\{Mn\}_{48hr}$, as a funtion of $\{Mn\}_i$ and $\{Pb\}_i$ in the bicarbonate buffered experiments after 48 hours.

Table 4: Amount of Mn precipitated and final pH after 48 hours in borate and bicarbonate buffered experiments based on an average of 3 measurements (1 standard deviation is given in parentheses). $\{Pb\}_i$ = 3 mg/L is average of six measurements.

**$\{Mn\}_i - \{Mn\}_{48hr}$ for borate buffered experiments:**

| $\{Mn\}_i$ (mg/L) | $\{Pb\}_i$ = 3 mg/L experiments | Final pH | $\{Pb\}_i$ = 1 mg/L experiments | Final pH | $\{Pb\}_i$ = 0.3 mg/L experiments | Final pH | $\{Pb\}_i$ = 0 mg/L experiments | Final pH |
|---|---|---|---|---|---|---|---|---|
| 100 | 20.37 (8.24) | 7.95 | 25.62 (5.75) | 7.90 | 29.72 (3.46) | 7.85 | 23.81 (1.21) | 8.12 |
| 30 | 13.13 (4.11) | 8.20 | 15.81 (4.85) | 8.15 | 9.52 (3.23) | 8.16 | 8.97 (4.85) | 8.28 |
| 10 | 5.10 (1.06) | 8.31 | 5.60 (1.78) | 8.30 | 4.63 (1.31) | 8.31 | 3.24 (0.1) | 8.39 |
| 3 | 2.27 (1.02) | 8.40 | 1.41 (0.29) | 8.39 | 0.48 (0.06) | 8.38 | <0.35 | 8.42 |
| 1 | 0.75 (0.27) | 8.42 | 0.54 (0.05) | 8.40 | <0.35 | 8.40 | <0.35 | 8.42 |

**$\{Mn\}_i - \{Mn\}_{48hr}$ for bicarbonate buffered experiments:**

| $\{Mn\}_i$ (mg/L) | $\{Pb\}_i$ = 3 mg/L experiments | Final pH | $\{Pb\}_i$ = 1 mg/L experiments | Final pH | $\{Pb\}_i$ = 0.3 mg/L experiments | Final pH | $\{Pb\}_i$ = 0 mg/L experiments | Final pH |
|---|---|---|---|---|---|---|---|---|
| 100 | 19.47 (4.63) | 7.60 | 13.23 (3.65) | 7.61 | 11.89 (4.30) | 7.50 | 7.22 (3.22) | 7.41 |
| 30 | 5.39 (2.70) | 7.85 | 10.46 (6.70) | 7.71 | 6.61 (1.07) | 7.75 | 5.61 (3.12) | 7.75 |
| 10 | 3.43 (1.27) | 8.00 | 2.38 (0.23) | 8.00 | 2.70 (0.59) | 7.95 | 1.39 (0.63) | 8.01 |
| 3 | 1.37 (0.83) | 8.10 | 0.72 (0.10) | 8.21 | 0.88 (0.09) | 8.25 | 0.45 (0.01) | 8.31 |
| 1 | 0.54 (0.29) | 8.20 | 0.38 (0.03) | 8.27 | <0.35 | 8.35 | <0.35 | 8.31 |

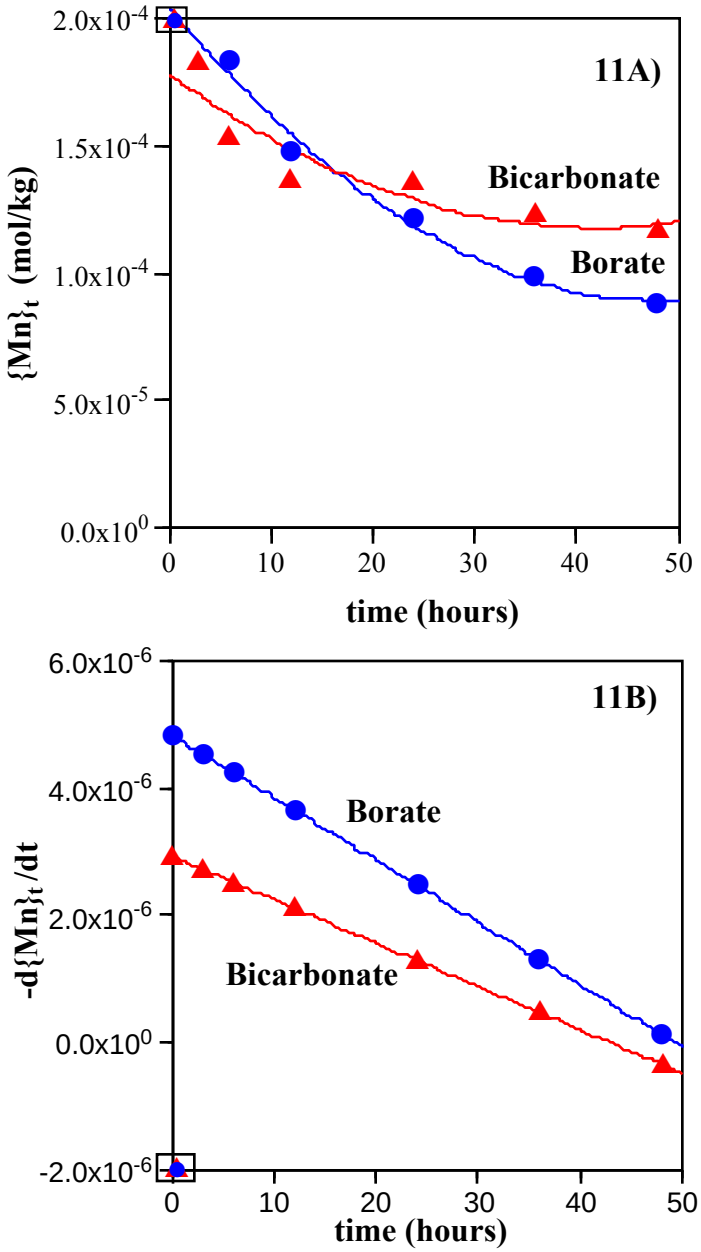


Figure 11: Removal of Mn from solution as a function of time. A) Change in $\{Mn\}_t$ as a function of time with a second order polynomial fit of the data. The derivative of the fit gives $d\{Mn\}_t/dt = 9.8x10^{-8}\ t - 4.8x10^{-6}$ with $r^2 = 0.98$ for the borate bufferd experiments and $d\{Mn\}t/dt = 6.8x10^{-8}\ t - 2.9x10^{-6}$ with $r^2 = 0.85$ for the bicarbonate experiments. B) Change in $d\{Mn\}_t/dt$ as a function of time. The derivative of the linear regression gives the rate, $r = 9.8x10^{-8}\ t - 4.8x10^{-6}$ with $r^2 = 1.00$ for the borate buffered experiments and $r = 6.8x10^{-8}\ t - 2.9x10^{-6}$ with $r^2 = 1.00$ for the bicarbonate buffered experiments. ▲ denotes the rate at the start of the experiments.

used to approximate the concentration versus time behavior in Figure 11a. The derivative of this polynomial was evaluated at each time interval with measured concentrations to produce a time specific rate ($d\{Mn\}_t/dt$). The rate of Mn precipitation over the 48 hour time frame of these experiments is shown in Figure 11b. The derivative of the regression for these points produces the rate of precipitation. This process produced a Mn precipitation rate of $9.8 \times 10^{-8}$ mol $kg^{-1}$ $sec^{-1}$ for the borate buffered experiments and $6.8 \times 10^{-8}$ mol $kg^{-1}$ $sec^{-1}$ for the bicarbonate buffered experiments. These data were then recast by plotting $\log\{Mn\}_t$ as a function of time to determine the rate constant k (calculations are in Appendix 4). This rate constant was used to compare the rates determined in this study with the rates of Davies and Morgan (1989) who also used silica as a substrate for Mn precitation. The rate constant in the borate buffered experiments is $2.9 \times 10^{-4}$ $min^{-1}$ and $1.4 \times 10^{-4}$ $min^{-1}$ in the bicarbonate buffered experiments. The two rates from this study can then be compared to $1.5 \times 10^{-4}$ $min^{-1}$ in the work by Davies and Morgan (1989). The comparison is discussed in Chapter 4.

# CHAPTER 4: DISCUSSION

The white precipitate that formed when the Pb reagent was added to the buffer solutions shows that the Pb is initially present as a suspended solid. In addition, these Pb precipitates were not initially associated with the quartz surfaces because no Pb was found to be present on the quartz surfaces before 12 hours of reaction (see Figure 7). Therefore, these Pb precipitates are probably initially suspended in solution (up to at least 6 hours). In the borate buffered experiments, this precipitate is probably $PbB_2O_4 \bullet H_2O$ as identified by XRD. Also, the white precipitate was observed to form as the Pb reagent was pipetted into the borate buffer solution. When the Pb reagent is added to the buffer solution, the solution is locally supersaturated with respect to this Pb-borate phase (see Figure 12). The reaction is:

$$Pb^{2+} + 2H_3BO_3 = PbB_2O_4 \bullet H_2O + 2H^+ + H_2O$$

However, once the solutions are completely mixed, the final solution is undersaturated with respect to Pb-borate and supersaturated with respect to hydrocerrusite [$(Pb_3(CO_3)_2(OH)_2$]. Hydrocerrusite precipitates according to the reaction:

$$3Pb^{2+} + 2HCO_3^- + 2H_2O = (Pb_3(CO_3)_2(OH)_2 + 4H^+$$

Because hydrocerrusite is also present in the borate buffered experiments some of the Pb-borate phase must re-dissolve and re-precipitate as hydrocerrusite. However, borate is not present in the bicarbonate buffered experiments so only hydrocerrusite precipitates, as indicated by the XRD results. These hydrocerrusite precipitates were also initially suspended in solution and not associated with the quartz grains (see Figure 7).

The discovery of an initial Pb-precipitate is not surprising because earlier studies on coprecipitation of Mn oxyhydroxides and heavy metals typically found that the metals

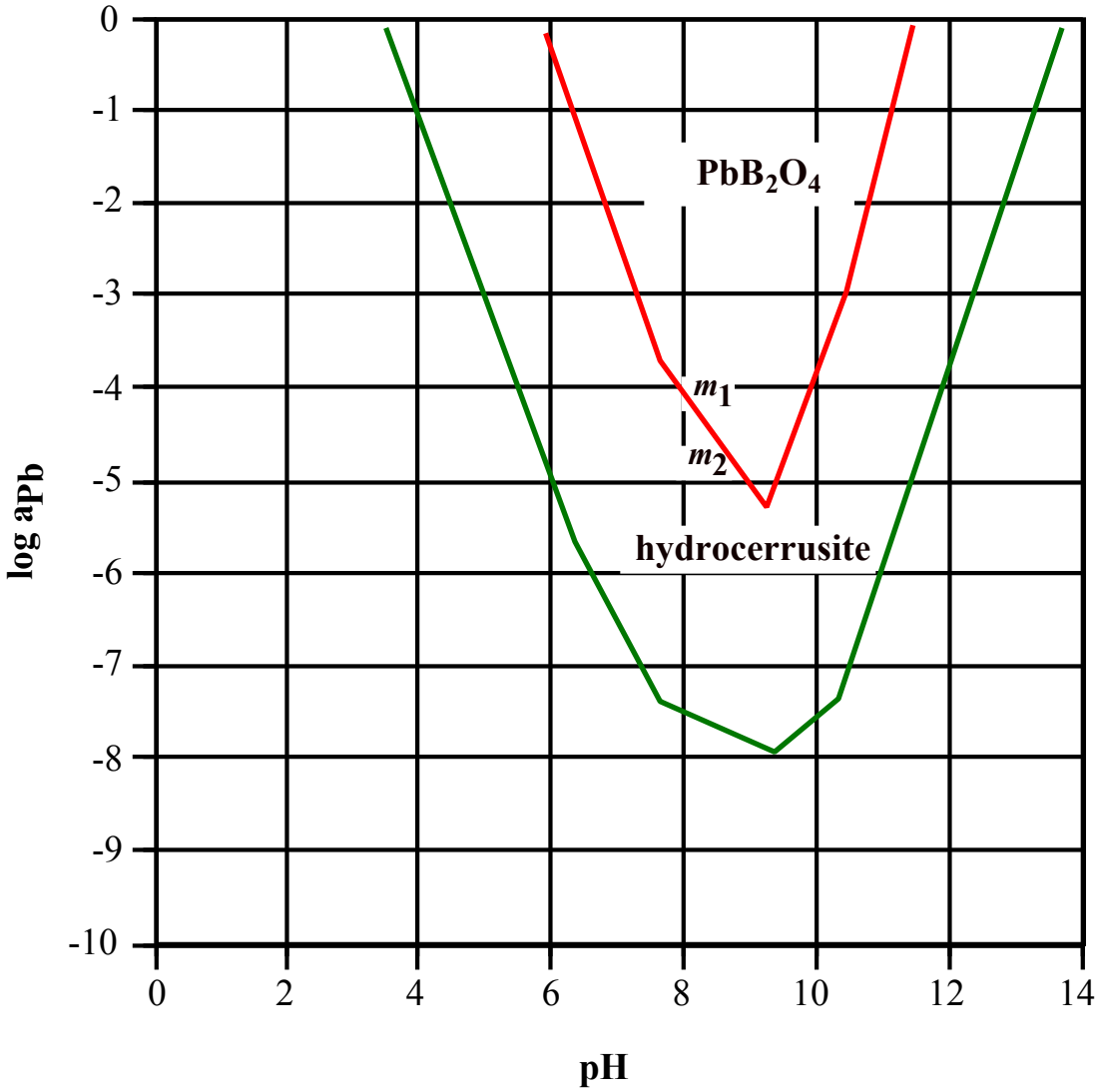


Figure 12: $PbB_2O_4$ solubility with total borate of 0.01 molal and hydrocerrusitesolubility with total carbonate of $3.2 \times 10^{-4}$ molal. These solubilities represent the conditions in the borate buffered experiments. Total carbonate was $1.2 \times 10^{-3}$ molal and Total borate was 0 molal in the bicarbonate buffered experiments. The hydrocerrusite stability field is therefore larger than shown above in the bicarbonate buffered experiments. $m_1$ denotes local concentration of experimental solution upon addition of the Pb reagent and $m_2$ denotes concentration of experimental solutions with $\{Pb\}_i$ = 3 mg/L after mixing.

precipitate as hydroxides and/ or carbonates (e.g. CoOOH, $CdCO_3$) before they are incorporated into the Mn oxyhydroxides (Matsui, 1973; Hem et al., 1989; Hem and Lind, 1991). Such behavior is also likely in natural waters, which often contain enough bicarbonate to cause the precipitation of metal hydroxycarbonates whenever the pH is increased to initiate Mn oxyhydroxide precipitation.

This study was unable to identify the mineralogy of the precipitated Mn oxyhydroxides using XRD because the Mn oxyhydroxide did not produce an X-ray pattern. However, XPS analysis showed that the Mn in the precipitates is predominantly in the 3+ oxidation state and Junta and Hochella (1994) found that $Mn^{3+}$ oxyhydroxides precipitating on hematite and albite surfaces were feitknechtite (β-MnOOH). In addition, the tiny Mn oxyhydroxide crystallites that were observed in this study (see Figure 2) are very similar to the habit of the feitknechtite precipitates in the study by Junta and Hochella (1994). Because the incubation time in this study was only 48 hours, most likely the $Mn^{3+}$ precipitates on the quartz sand is an X-ray amorphous precursor of feitknechtite or some other Mn3+-bearing oxyhydroxide. Our results are similar to those of Hem (1980) who also found, in Pb and Mn coprecipitation experiments, that the initial Mn oxyhydroxide precipitates were X-ray amorphous.

It appears that $PbB_2O_4 \bullet H_2O$ and hydrocerrusite act as a substrate for the nucleation of Mn oxyhydroxides. This could occur because the Mn oxyhydroxides overgrow the suspended Pb particles and isolate them from further reaction with the solution. The suspended Pb particles appear to form as the reagents are mixed for both experiments and are certainly present within 3 hours of reaction time. In some of the experiments ($\{Mn\}_i$ < 30 mg/L) Mn precipitation does not occur until at least 3 hours. As the Mn oxyhydroxides continue to grow on the Pb-

precipitate surfaces, it appears that they are attracted to silica surfaces (quartz sand and the walls of glass flasks). This occurs because the net negatively charged quartz surface at pH 8.5 (Zero point of charge = 1-2 from Parks, 1965; 1967) attracts the net positively charged Mn oxyhydroxide surface. Mn oxyhydroxides most likely have a zero point of charge greater then 9 since oxyhydroxides of Al and $Fe^{3+}$ generally have values above 9 (Parks, 1965; 1967). When the colloidal Mn oxyhydroxides attach to the quartz surface, they carry along the Pb-precipitates and remove them from solution. These attached particles are then overgrown by additional Mn oxyhydroxides, trapping the Pb precipitates to the surface and shielding the Pb from further interaction with solution. However, in borate and bicarbonate buffered experiments with $\{Mn\}_i$ > 30 mg/L, $Q_{Pb}$ decreases (see Figure 7) relative to experiments with $\{Mn\}_i$ < 30 mg/L. This is probably due to direct nucleation of Mn oxyhydroxides on the quartz surface because in experiments with $\{Pb\}_i$ = 0 mg/L, Mn oxyhydroxides have clearly grown on quartz surfaces (see Figure 1). Growth of Mn oxyhydroxides on the surface changes the quartz surface to a net positive charge and repels the remaining suspended Mn-coated Pb colloids. Therefore, this growth reduces $Q_{Pb}$ and results in the suspended Mn precipitates that were observed in experiments with $\{Mn\}_i$ > 30 mg/L.

The acetic acid leaching procedure showed that Mn is leached from the Mn oxyhydroxide phases formed in both the borate and bicarbonate buffered experiments. However, detectable extractable lead ($E_{Pb}$) was only found in the leachate from the bicarbonate buffered experiments, ranging from 35-100% of $Q_{Pb}$. $E_{Mn}$ in the borate and bicarbonate buffered experiments appears to be directly related to the $Q_{Mn}$ (see Figure 9). Because much more Mn is precipitated on the surfaces in the borate buffered experiments, it appears that the Mn oxyhydroxides shield the Pb

from the leaching solutions. Therefore, greater amounts of precipitated Mn provides a better retention capability for Pb.

It appears that a Pb-Mn mixed oxide has not yet formed at the end of the 48 hour experiments because Pb is leached from the quartz grains from the bicarbonate buffered experiments and Pb retention in the borate buffered experiments appears to be the result of shielding by the overgrown Mn oxyhydroxides. In addition, $Mn^{3+}$ is the dominant valence state after 48 hours of reaction (see Figure 3) and Hem et al. (1989; 1991) determined that all the Mn was in the 4+ oxidation state for mixed Mn/metal oxides. The absence of an initial Mn/metal oxide is consistent with previous coprecipitation studies, where mixed Mn/metal oxides did not precipitate initially (Matsui, 1973; Hem et al., 1985; Hem and Lind, 1991). These studies also suggest that a metal coprecipitate forms initially and that a Mn/metal compound (e.g. $Cd_2Mn_3O_8$) forms only after aging and further Mn oxidation to $Mn^{4+}$. Formation of a mixed Pb/Mn oxyhydroxide could have occurred in the borate buffered experiments after 60 days because XPS data confirms that Mn oxyhydroxides contain some $Mn^{4+}$. Further study to determine how the $Q_{Pb}/Q_{Mn}$ ratios change with increasing $E_{Mn}$ and to identify surface precipitates would have to be undertaken before any conclusions can be made. Our results and previous coprecipitation studies suggest that $Mn^{4+}$ will form as the precipitate ages and that $Mn^{4+}$ oxides are more structurally suitable for cation incorporation (Giovanoli and Balmer, 1981; Post et al., 1982). Therefore, the Mn oxyhydroxides analyzed after 60 days should possess a stronger capability for Pb incorporation and retention.

This study clearly demonstrates that the amount of Mn precipitation and therefore the Pb retention capacity is enhanced in the borate buffered experiments. In addition, the Mn

precipitation rate is 1.5 times higher in the borate buffered experiments than in the bicarbonate buffered experiments. Most likely, this is due to the stronger buffer capacity of borate buffered solutions as shown by the higher final pH readings of the borate buffered experiments (see Table 4). This result agrees with Morgan (1967) who has shown that Mn precipitation is strongly dependent on pH. Another contributing factor to the slower rate in the bicarbonate buffered experiments is the presence of $HCO_3^-$. Previous studies have shown that $MnHCO_3^+$ is an important and strong complex in natural waters (Hem, 1963a; Morgan, 1967). Hem (1963a) has also shown that the presence of $HCO_3^-$ inhibits the Mn precipitation rate. Finally, the Pb-borate phase may have a stronger nucleation effect on Mn precipitation. Studies have shown that various substrates influence Mn oxidation rates differently (Coughlin and Matsui, 1976; Davies and Morgan, 1989). The increase in Mn precipitation and precipitation rate in the borate buffered experiments leads to significantly more Mn (up to 19% more) precipitated onto quartz surfaces over the 48 hour duration of these experiments. In addition, the $Q_{Pb}/Q_{Mn}$ ratios are lower in the borate buffered experiments because relatively more Mn has been precipitated on these surfaces. The results of this study also indicate that $Q_{Pb}$ is significantly increased in the borate buffered experiments. This is probably related to the increase in Mn oxyhydroxides precipitated on the suspended Pb-borate particles since Mn growth traps the Pb colloid to the quartz surface.

The presence of borate is not the only contributing factor to increased Mn precipitation in this system. Increased $\{Mn\}_i$ and increased $\{Pb\}_i$ also enhance Mn precipitation (see Figure 10). These trends are consistent with previous studies that have shown that increasing Mn concentration and metal concentration intensifies Mn precipitation (Matsui, 1973; Hem, 1981; Hem and Lind, 1991). However, data from experiments with $\{Mn\}_i$ = 100 mg/L are not

consistent with this trend. These data were not plotted because this extreme concentration of Mn is improbable in natural settings and the high concentration of Mn changes the system in a manner these experiments were not designed to test. These data do suggest that the positive effect of increased $\{Mn\}_i$ does have an upper limit but further study is needed before conclusions can be drawn. Finally, there is significant error associated with these data, and the scatter can be attributed to experimental procedures including potential inconsistencies in cleaning the glass flasks and differences in wall surfaces of the glass flasks (e.g. abundance of scratches). Because the from the $\{Mn\}_i < 30$ ppm experiments data are consistent with earlier studies and the observed trends are probably real.

When the Mn precipitation rates are recast to compare with Mn precipitation rates on silica substates in the work by Davies and Morgan (1989), the precipitation rate in the borate buffered experiments is twice as fast. However, because of the presence of suspended Pb precipitates in the solution during Mn precipitation, the determination of surface area is near impossible. So, for the comparison, surface area was assumed to be the same in both studies. If the surface area were much greater in this study than the rates in Davies and Morgan (1989) would be faster. Determining the changing surface area as Mn oxyhydroxides precipitate continues to be an unresolved problem in precipitation rate determination. Resolving this problem was beyond the scope of this project, but it should be investigated by future research.

Because precipitation of Mn and Pb onto quartz surfaces and retention of Pb during leaching conditions has been demonstrated, coprecipitation of Mn oxyhydroxides with Pb is a potential remediation technique for aqueous systems contaminated with Pb. A potential scenario for such a process is that contaminated aqueous solutions would be first dosed with $Mn^{2+}$, if

needed, and a borate buffer and then circulated through a bed of quartz sand grains. Coprecipitation would be catalyzed initially by the borate buffer. These additions would raise the pH and Mn concentrations to optimal conditions for Mn precipitation and greatly enhance the rate of Mn (and Pb) precipitation onto the quartz sand surfaces. Once the sand grains are coated (< 24 hours), the borate buffer could be replaced with a bicarbonate buffer since $HCO_3^-$ is of significantly less environmental concern and much less expensive. Although there are currently no regulations for boron, it is under consideration for regulation by the EPA (EPA, 1998). Carriker and Brezonik (1978) state that dissolved boron is not toxic to humans and animals at concentrations of less than 30 mg/L. Boron concentrations in discharge effluent from the remediation system should be kept around this level pending regulation. However, Van der Weijden (1975) has shown that Mn-oxide substrates have the strongest catalytic effect on Mn oxyhydroxide precipitation, and so replacing the borate buffer after the sand grains are coated with Mn oxyhydroxides should not reduce the ability of the system to scavenge Pb. Once monitoring reveals the Pb has been effectively removed from the system, the sand grains would be allowed to age in solution, further enhancing their metal retention capability before proper disposal. If time of remediation was a serious concern, the borate buffer could be used throughout the remediation process. Because the Pb-borate precipitate nucleates Mn oxyhydroxides in this system, some of the borate will be trapped at the quartz surface with the Pb. If further study indicated that the borate in the discharge effluent was below any future regulations and that it was retained by the Mn oxyhydroxides, then the borate buffer could be used for the entire remediation procedure.

# CHAPTER 5: CONCLUSIONS

Coprecipitation of Pb with Mn oxyhydroxides in the presence of a borate buffer, a bicarbonate buffer, and a quartz substrate was studied to investigate the scavenging capacity of Mn oxyhydroxides. The results indicate that initially, hydrocerrusite and $PbB_2O_4 \bullet H_2O$ grow in suspension in the borate buffered experiments and hydrocerrusite forms in suspension in the bicarbonate buffered experiments. Mn oxyhydroxides then nucleate on these suspended Pb precipitates in both experiments with Mn precipitation significantly enhanced in the borate buffered experiments. As the Mn oxyhydroxides grow on the Pb precipitate surfaces, these particles are attracted to quartz sand surfaces. This process carries the Pb precipitates to the quartz surface where they adhere and are overgrown by further Mn precipitation. These Mn oxyhydroxides trap the Pb and form a barrier that shields the Pb from further interaction with solution. Leaching studies show that Pb is strongly retained ($E_{Pb} = 0$) in the borate precipitated Mn oxyhydroxides while it is less well retained for the bicarbonate precipitated Mn oxyhydroxides. It is likely that the superior Pb retention capacity of the Mn oxyhydroxides in the borate buffered experiments is due to the increased amount of Mn precipitated onto the surface.

These results strongly suggest that Pb coprecipitation with Mn oxyhydroxides will effectively remove Pb from solution and will retain it through pH 5 leaching conditions. This coprecipitation process has potential for remediating Pb contaminated aqueous solutions and could provide an effective tool for remediation of many other toxic metals. Not only will this mechanism remove aqueous $Pb^{2+}$ from solution but it appears it will also substantially incorporate colloidal Pb particles as well.

## REFERENCES


Alloway B. J. (1995) Soil processes and the behavior of metals. In *Heavy metals in soils*, *2nd ed.* (B. J. Alloway, Ed.), Blackie Academic and Professional, London: 368 pp.

Carlos B. A., Chipera S. J., Bish D. L., and Craven S. J. (1993) Fracture-lining manganese oxide minerals in silicic tuff, Yucca Mountain, Nevada, U.S.A. *Chem. Geol.* **107**: 47-69.

Carpenter R. H. and Hayes W. B. (1978) Precipitation of iron, manganese, zinc, and copper on clean, ceramic surfaces in a stream draining a poly-metallic sulfide deposit. *J. Geochem. Explor.* **9**: 31-37.

Carpenter R. H., Robinson G. D., and Hayes W. B. (1978) Partitioning of manganese, iron, copper, zinc, and nickel in black coatings on stream boulders in the vicinity of the Magruder Mine, Lincoln County, Georgia. *J. Geochem. Explor.* **10**: 75-89.

Carpenter R. H., Pope T. A., and Smith R. L. (1975) Fe-Mn oxide coatings in stream sediment geochemical surveys. *J. Geochem. Explor.* **4**: 349-363.

Carriker N. E. and Brezonik P. L. (1978) Sources, levels, and reactions of boron in Florida waters. *J. Environ. Qual.* **7**: 516-522.

Chao T. T. and Anderson B. J. (1974) The scavenging of silver by manganese and iron oxides in stream sediments collected from two drainage areas of Colorado. *Chem. Geol.* **14**: 159-166.

Coughlin R. W. and Matsui I. (1976) Catalytic oxidation of aqueous Mn(II). *J. Catalysis* **41**: 108-123.

Crerar D. A. and Barnes H. L. (1974) Deposition of deep-sea manganese nodules. *Geochim. Cosmochim. Acta* **38**: 279-300.

Davies S. H. R. and Morgan J. J. (1989) Manganese (II) oxidation kinetics on metal oxide surfaces. *J. Colloid Interface Sci.* **129**: 63-77.

Dillard J. G., Crowther D. L., and Murray J. W. (1982) The oxidation states of cobalt and selected metals in Pacific ferromanganese nodules. *Geochim. Cosmochim. Acta* **46**: 755-759.

Giovanoli R. And Balmer B. (1981) A new synthesis of Hollandite. A possibility for immobilization of nuclear waste. *Chimia* **35**: 53-55.

Hem J. D. (1963a) Chemical equilibria and rates of manganese oxidation. *USGS Water Supply Paper* **1667-A**: A1-A64.

Hem J. D. (1963b) Increased oxidation rate of manganese ions in contact with feldspar grains. *USGS Professional Paper* **475-C**: C216-C217.

Hem J. D. (1980) Redox coprecipitation mechanisms of manganese oxides. In *Particulates in Water: Characterization, Fate, Effects, and Removal* (M. C. Kavanaugh and J. O. Leckie, Eds.); Advances in Chemistry Series **189**: 45-72. American Chemical Society.

Hem J. D. (1981) Rates of manganese oxidation in aqueous systems. *Geochim. Cosmochim. Acta* **45**: 1369-1374.

Hem J. D. and Lind C. J. (1983) Nonequilibrium models for predicting forms of precipitated manganese oxides. *Geochim. Cosmochim. Acta* **47**: 2037-2046.

Hem J. D. and Lind C. J. (1991) Coprecipitation mechanisms and products in manganese oxidation in the presence of cadmium. *Geochim. Cosmochim. Acta* **55**: 2435-2451.

Hem J. D., Lind C. J., and Roberson, C. E. (1989) Coprecipitation and redox reactions of manganese oxides with copper and nickel. *Geochim. Cosmochim. Acta* **53**: 2811-2822.

Hem J. D., Roberson C. E., and Lind C. J. (1985) Thermodynamic stability of CoOOH and its coprecipitation with manganese. *Geochim. Cosmochim. Acta* **49**: 801-810.

Hem J. D., Roberson C. E., and Lind C. J. (1987) Synthesis and stability of hetaerolite, $Zn_2Mn_3O_8$, at 25°C. *Geochim. Cosmochim. Acta* **51**: 1539-1547.

Jenne E. A. (1968) Controls on Mn, Fe, Co, Ni, Cu, and Zn concentrations in soils and water: the significant role of hydrous Mn and Fe oxides. In *Trace inorganics in water*, Advances in Chemistry Series **73**: 337-387. American Chemical Society.

Junta J. L. and Hochella M. F., Jr. (1994) Manganese (II) oxidation at mineral surfaces: A microscopic and spectroscopic study. *Geochim. Cosmochim. Acta* **58**: 4985- 4999.

Lind C. J. And Hem J. D. (1993) Manganese minerals and associated fine particulates in the streambed of Pinal Creek, Arizona, U.S.A.: a mining-related acid drainage problem. *Applied Geochem.* **8**: 67-80.

Loganathan P. and Burau R. G. (1973) Sorption of heavy metal ions by a hydrous manganese oxide. *Geochim. Cosmochim. Acta* **37**: 1277-1293.

Matsui I. (1973) Catalysis and kinetics of manganous ion oxidation in aqueous solution and adsorbed on the surfaces of solid oxides. Ph. D. Dissertation, Lehigh Universtiy: 221 pp.

Morgan J. J. (1967) Chemical equilibria and kinetic properties of manganese in natural waters. In *Principles and Applications of Water Chemistry* (S. Faust and J. Hunter, Eds.): 561-624. John Wiley & Sons, Inc.

Morgan J. J. and Stumm W. (1965) *J. Amer. Water Works Assoc.* **57**: 107-119.

Murray J. W., Dillard J. G., Giovanoli R., Moers H., and Stumm W. (1985) Oxidation of Mn(II): Initial mineralogy, oxidation state and ageing. *Geochim. Cosmochim. Acta* **49**: 463-470.

Nraigu J. O. and Pacyna J. M. (1988) Quantitative assessment of worldwide contamination of air, water and soils by trace metals. *Nature* **333**: 134-139.

Parks G. A. (1965) The isoelectric points of solid oxides, solid hydroxides, and aqueous hydroxo complex systems. *Chem. Rev.* **65**: 177-198.

Parks G. A. (1967) Aqueous surface chemistry of oxides and complex oxide minerals: Isoelectric point and zero point of charge. In: Equilibrium concepts in natural water systems (W. Stumm, ed.): 121-160. American Chemical Society.

Post J. E., Von Dreele R. B., and Buseck P. R. (1982) Symmetry and cation displacments in hollandites. Structure refinements of hollandite, cryptomelane, and priderite. *Acta Cryst.* **B38**: 1056-1065.

Robinson G. D. (1981) Adsorption of Cu, Zn and Pb near sulfide deposits by hydrous manganese-iron oxide coatings on stream alluvium. *Chem. Geol.* **33**: 65-79.

Sung W. and Morgan J. J. (1981) Oxidative removal of Mn(II) from solution catalyzed by the γ-FeOOH (lepidcrocite) surface. *Geochim. Cosmochim. Acta* **45**: 2377-2383.

U. S. Environmental Protection Agency (1998) Drinking water contaminant candidate list. *EPA document* **815-F-98-002**: February 1998.

Van der Weijden C. H. (1975) Sorption experiments relevant to the geochemistry of manganese nodules. Ph. D. Dissertation, University Utrecht, 154 pp.

Wilson D. E. (1980) Surface and complexation effects on the rate of Mn(II) oxidation in natural waters. *Geochim. Cosmochim. Acta* **44**: 1311-1317.

Yeh J. J. and Lindau I. (1985) Atomic subshell photoionization cross sections and asymmetry parameters: $1 < Z < 103$. *Atomic Data and Nuclear Data Tables* **32**: 1-155.

## Appendix 1: Experimental Protocols

*Procedure for borate buffered experiments*

The following is the procedure for performing Mn precipitation experiments with a pH 8.5 boric acid buffer. These experiments were all run for 48 hours at 25°C and in a temperature-controlled shaker bath set at ~175 excursions/ minute.

Reagents:

- 0.01 *m* NaOH
- 0.1 *m* $H_3BO_3$
- $1.8x10^{-2}$ *m* $MnCl_2$
- $4.0x10^{-4}$ *m* $MnCl_2$
- $6.0x10^{-5}$ *m* $Pb(NO_3)_2$

Procedure:

1. Gather six 250 mL flasks, six 200 mL volumetrics, and six #6 rubber stoppers. Label each flask and volumetric (1 flask and 1 volumetric per run) with a sample number.

2. Weigh out 3 g of quartz grains for each flask from the HCl-rinsed quartz grains and place 3 g of quartz in each flask.

3. Pipette 36 mL of 0.01 *m* NaOH and 20 mL of 0.1 *m* $H_3BO_3$ into each 200 mL volumetric (six total per experiment).

4. Pipette the following volumes of $MnCl_2 \bullet 4H_2O$[1] into the appropriate 200 mL volumetric:
- Volumetric #1: 24 mL of $1.8x10^{-2}$ *m* $MnCl_2$ ($\{Mn\}_i = 100$ mg/L)
- Volumetric #2: 7.3 mL of $1.8x10^{-2}$ *m* $MnCl_2$ ($\{Mn\}_i = 30$ mg/L)
- Volumetric #3: 20 mL of $4.0x10^{-4}$ *m* $MnCl_2$ ($\{Mn\}_i = 10$ mg/L)
- Volumetric #4: 6 mL of $4.0x10^{-4}$ *m* $MnCl_2$ ($\{Mn\}_i = 3$ mg/L)
- Volumetric #5: 2 mL of $4.0x10^{-4}$ *m* $MnCl_2$ ($\{Mn\}_i = 1$ mg/L)
- Volumetric #6: 0 mL of $4.0x10^{-4}$ *m* $MnCl_2$ ($\{Mn\}_i = 0$ mg/L)

5. Pipette 60-90 mL of D.D.I. water into each volumetric (volume of water depends on the volume of $MnCl_2$ used).

6. Depending on the desired initial $Pb^{2+}$ concentration pipette the following volume of $6.0x10^{-5}$ *m* $Pb(NO_3)_2$ into all six volumetrics:

---

[1] The $MnCl_2 \bullet 4H_2O$ solid is hygroscopic. The calculated concentration was $1.8 \times 10^{-2}$ *m* but the actual concentration was determined by the colorimetric method. Therefore, the recipe for 100 and 30 mg/L initial $Mn^{2+}$ ranged from 20-24 mL and 6-8 mL, respectively.

## Appendix 1: Experimental Protocols

- for $\{Pb\}_i$ = 3 mg/L, pipette 30 mL of $6.0 \times 10^{-5}$ *m* $Pb(NO_3)_2$
- for $\{Pb\}_i$ = 1 mg/L, pipette 10 mL of $6.0 \times 10^{-5}$ *m* $Pb(NO_3)_2$
- for $\{Pb\}_i$ = 0.3 mg/L, pipette 3 mL of $6.0 \times 10^{-5}$ *m* $Pb(NO_3)_2$
- for $\{Pb\}_i$ = 0 mg/L initial, pipette 0 mL of $6.0 \times 10^{-5}$ *m* $Pb(NO_3)_2$

7. Fill each volumetric to volume and mix well.

8. Transfer the solution to 250 mL glass flasks and mix thoroughly. Record the pH, start time, and date of each run.

9. Cork each flask and place them in a shaker bath at 25°C and ~175 excursions/ minute.

10. Before the end of the experiment, weigh and label sample bottles (30 mL plastic).

11. At the end of each experiment, remove the flasks from the shaker bath and measure final pH. Record time, date, and final pH.

12. Fill sample bottles with ~30 mL solution from each of the runs, and weigh.

13. Rinse the quartz grains in each flask three times with D.D.I. water. After each rinse, swirl the flask vigorously. Discard the supernatant after each rinse.

14. Dry the quartz grains at 60°C. Once the quartz grains have dried, store the grains in labeled glass vials for future analysis.

15. Analyze the solutions from all the runs for $\{Mn\}_{48hr}$ and $\{Pb\}_{48hr}$ as described below.

16. The following dilutions are needed for Mn analysis while none are necessary for Pb analysis:

    a. $\{Mn\}_i$ = 100 mg/L: pipette 5 mL of sample into a 100 mL volumetric and make to volume. Then pipette 10 mL of the diluted sample into a 25 mL volumetric.

    b. $\{Mn\}_i$ = 30 mg/L: pipette 10 mL of sample into a 50 mL volumetric and make to volume. Then pipette 10 mL of the diluted sample into a 25 mL volumetric.

    c. $\{Mn\}_i$ = 10 mg/L: pipette 5 mL of sample into a 10 mL volumetric and make to volume. Then pipette 10 mL of the diluted sample into a 25 mL volumetric.

    d. For the $\{Mn\}_i$ = 3 mg/L and 1 mg/L: add 10 mL of the solution directly to a 25 mL volumetric.

## Appendix 1: Experimental Protocols

*Procedure for bicarbonate buffered experiments*

The following is the procedure for experiments with a pH 8.5 sodium bicarbonate/ sodium carbonate buffer. These experiments all ran for 48 hours at 25°C and in a temperature-controlled shaker bath set at ~65 excursions/ minute.

Reagents:

- 0.01 *m* $NaHCO_3$
- $1.65 \times 10^{-3}$ *m* $Na_2CO_3$
- $1.8 \times 10^{-2}$ *m* $MnCl_2$
- $4.0 \times 10^{-4}$ *m* $MnCl_2$
- $6.0 \times 10^{-5}$ *m* $Pb(NO_3)_2$
- $1.3 \times 10^{-3}$ *m* HCl

Procedure:

1. Gather six 250 mL flasks, six 200 mL volumetrics, and six #6 rubber stoppers. Label each flask and volumetric (1 flask and 1 volumetric per run) with a sample number.

2. Weigh out 3 g of quartz grains for each flask from the HCl-rinsed quartz grains and place 3 g of quartz in each flask.

3. Pipette the following volumes of $MnCl_2$ into the appropriate 200 mL volumetric:
- Volumetric #1: 24 mL of $1.8 \times 10^{-2}$ *m* $MnCl_2$ ($\{Mn\}_i = 100$ mg/L)
- Volumetric #2: 7.3 mL of $1.8 \times 10^{-2}$ *m* $MnCl_2$ ($\{Mn\}_i = 30$ mg/L)
- Volumetric #3: 20 mL of $4.0 \times 10^{-4}$ *m* $MnCl_2$ ($\{Mn\}_i = 10$ mg/L)
- Volumetric #4: 6 mL of $4.0 \times 10^{-4}$ *m* $MnCl_2$ ($\{Mn\}_i = 3$ mg/L)
- Volumetric #5: 2 mL of $4.0 \times 10^{-4}$ *m* $MnCl_2$ ($\{Mn\}_i = 1$ mg/L)
- Volumetric #6: 0 mL of $4.0 \times 10^{-4}$ *m* $MnCl_2$ ($\{Mn\}_i = 0$ mg/L)

5. Pipette 100 mL of D.D.I. water into each volumetric.

6. Depending on the desired initial $Pb^{2+}$ concentration pipette the following volume of $6.0 \times 10^{-5}$ *m* $Pb(NO_3)_2$ into all six volumetrics:
- for $\{Pb\}_i = 3$ mg/L, pipette 30 mL of $6.0 \times 10^{-5}$ *m* $Pb(NO_3)_2$
- for $\{Pb\}_i = 1$ mg/L, pipette 10 mL of $6.0 \times 10^{-5}$ *m* $Pb(NO_3)_2$
- for $\{Pb\}_i = 0.3$ mg/L, pipette 3 mL of $6.0 \times 10^{-5}$ *m* $Pb(NO_3)_2$
- for $\{Pb\}_i = 0$ mg/L, pipette 0 mL of $6.0 \times 10^{-5}$ *m* $Pb(NO_3)_2$

3. Continuously agitate the solution using a magnetic stir bar and slowly add 25 mL of pH 9.5 $NaHCO_3$- $Na_2CO_3$ buffer solution through a burette.

4. Pipette the following volumes of $1.3 \times 10^{-3}$ *m* HCl acid into each volumetric to adjust the pH to ~8.5. The volumes are as follows:

- $\{Mn\}_i$ = 100 mg/L: no acid added
- $\{Mn\}_i$ = 30 mg/L: 3-8 mL of acid
- $\{Mn\}_i$ = 10 mg/L: 8-12 mL of acid
- $\{Mn\}_i$ = 3 mg/L: 12-14 mL of acid
- $\{Mn\}_i$ = 1 mg/L: 15-20 mL of acid
- $\{Mn\}_i$ = 0 mg/L: 15-20 mL of acid

5. Fill each volumetric to volume with D.D.I. water and transfer to the 250 mL glass flasks.

6. At the end of the experiment, follow steps 7-12 of the boric acid buffered system procedure.

## Appendix 1: Experimental Protocols

*$Mn^{2+}$ Analysis Procedure (Colorimetric method)*

The following outlines the colorimetric method of Morgan and Stumm (1965) used to analyze $Mn^{2+}$ concentrations in solution for this study.

Analysis reagents:

- 5 *m* NaOH
- 1000 ppm Fisherchemical® Mn reference solution
- formaldioxime reagent

Preparation of reagents:

1. Prepare a 5 M NaOH solution by dissolving 20 g of NaOH solid in 100 mL of D.D.I. water. Store the solution in a 250 mL polyethylene bottle.

2. Prepare a 100 mg/L working standard by adding 10 mL of the 1000 ppm Mn reference solution to a 100 mL volumetric. Pipette 3 mL and 1 mL of the working standard into 100 mL volumetrics to make a 3 mg/L and 1 mg/L standards, respectively. For standards less than 1 mg/L dilute the 1 mg/L standard in the analysis volumetric (25 mL) as described below.

3. Prepare the formaldioxime reagent by dissolving 20 g of hydroxylamine hydrochloride solid with 200 mL of D.D.I. water in a 500 mL volumetric. Mix well and then pipette 10 mL of 37% formaldehyde to the volumetric, and make to volume.

Analysis Procedure:

1. Allow the spectrophotometer to warm up for 30 minutes before each analysis. Set the spectrophotometer on absorbence and 450 nm wavelength for all analyses. Mix assays in 25 mL volumetrics.

2. Pipette 2 mL of the formaldioxime reagent into each 25 mL volumetric.

3. Pipette 10 mL of solution to be analyzed into appropriate volumetrics. Pipette the following amounts into the standard volumetrics:

3 mg/L working standard.: 10 mL of 3 mg/L standard.
1 mg/L working standard.: 10 mL of 1 mg/L standard.
0.5 mg/L working standard: 5 mL of 1 mg/L standard.
0.4 mg/L working standard: 4 mL of 1 mg/L standard.

4. Pipette 5 mL of 5 M NaOH into each 25 mL volumetric and make to volume with D.D.I. water.

5. Mix each volumetric thoroughly and allow for complete color change (~45 minutes).

6. Transfer appropriate volume from each volumetric to analysis cuvettes and analyze a blank, standards, and unknowns.

## Appendix 1: Experimental Protocols

*$Pb^{2+}$ analysis procedure*

Analysis Reagents:

- 1000 ppm Fisherchemical® Pb reference solution

Procedure:

1. Prepare standards of 4 mg/L, 2 mg/L, 1 mg/L, and 0.8 mg/L from the Pb reference solution (1000 ppm). Prepare a 100 mg/L working standard by pipette 10 mL of the 1000 ppm Pb reference solution into a 100 mL volumetric and fill to volume (100 mg/L Pb). Then use this 100 mg/L working standard solution to make standards:
- pipette 4 mL of working standard into a 100 mL volumetric: 4 mg/L standard
- pipette 2 mL of working standard into a 100 mL volumetric: 2 mg/L standard
- pipette 1 mL of working standard into a 100 mL volumetric: 1 mg/L standard
- pipette 0.8 mL of working standard into a 100 mL volumetric: 0.8 mg/L standard

2. Adjust AA to the appropriate settings:
- 7A° slitwidth
- 283.7 nm wavelength
- 5.0 mA lamp current

3. Analyze standards, record absorbence, and produce a calibration curve of abosrbence versus concentration.

4. Run unkonwns and determine concentration from calibration curve:
concentration = (absorbence - intercept)/ slope.

## Appendix 1: Experimental Protocols

*Mn/Pb precipitate digestion procedure*

The following procedure describes the digestion process for determining $Mn^{2+}$ and metal concentrations associated with quartz grain surfaces. Precipitates on the quartz grains were dissolved using this procedure and the resulting solution was analyzed for $Mn^{2+}$and $Pb^{2+}$ concentrations.

Digestion reagents:

Concentrated $HNO_3$ (17.1 *m*)

Digestion Procedure:
1. Dry the Mn-coated grains at 60°C, then place them in 125 mL flasks, and add 25 mL of D.D.I. water.

2. Pipette ~10 mL of concentrated $HNO_3$ into each flask and mix the solutions gently.

3. Place the flasks on a hot plate in a hood and heat very slowly until the cinnamon-brown precipitates have dissolved off the quartz surfaces and the solution is clear.

4. For samples with thick coatings of Mn precipitate increase the amount of concentrated $HNO_3$ added (up to 25 mL) to promote the digestion.

5. When digestion is complete, dilute the digestion solution to 200 mL and allow to cool before analysis.

6. Analyze solutions using analytical methods described above and in the Methods section.

## Appendix 1: Experimental Protocols

*Acetic acid/ sodium hydroxide leach procedure*

The following procedure describes the pH 5 leach test of Mn- coated quartz grains. Quartz grains with Mn precipitates on their surfaces were digested in a pH 5 HAc- NaOH buffered solution for 5 hours at 25°C. The solution was then analyzed for Mn and metal concentrations.

Leach reagents:

- 1 *m* acetic acid (Hac)
- 1 *m* sodium hydroxide (NaOH)

Leach procedure:

1. Combine 165 mL of 1 m HAc and 10 mL of 1 m NaOH in a 1000 mL volumetric and fill to volume with D.D.I. water. This is the pH 5 HAc- NaOH buffer.

2. Place dried, Mn- coated, quartz grains in labeled 250 mL glass flasks.

3. Pipette 75 mL of pH 5 HAc- NaOH buffer into each flask.

4. Cork the flasks and plac them in a shaker bath at 25°C. Set the speed to ~65 excursions/ minute.

5. Agitate the samples for five hours.

6. After five hours, measure final pH and decant solution into 200 mL volumetric.

7. Analyze solutions using the procedures described above and in the Methods section.

**Appendix 1: Calibration curves for solution analysis methods**

A) Typical calibration curve for Pb by Acetylene-flame Atomic Absorption (AA)

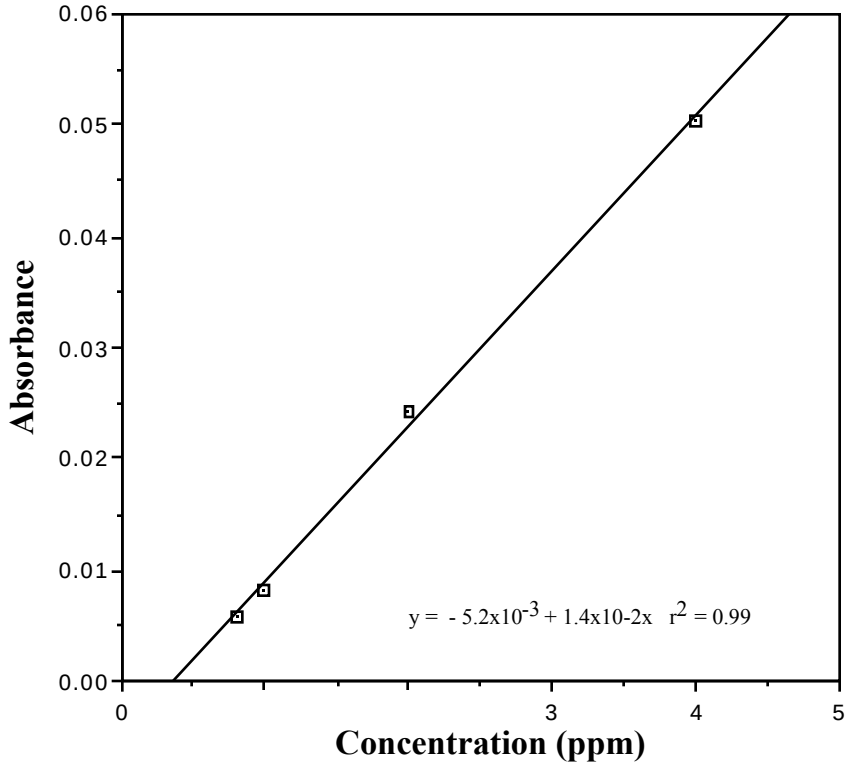


B) Typical calibration curve for formaldioxime colorimetric method (Mn)

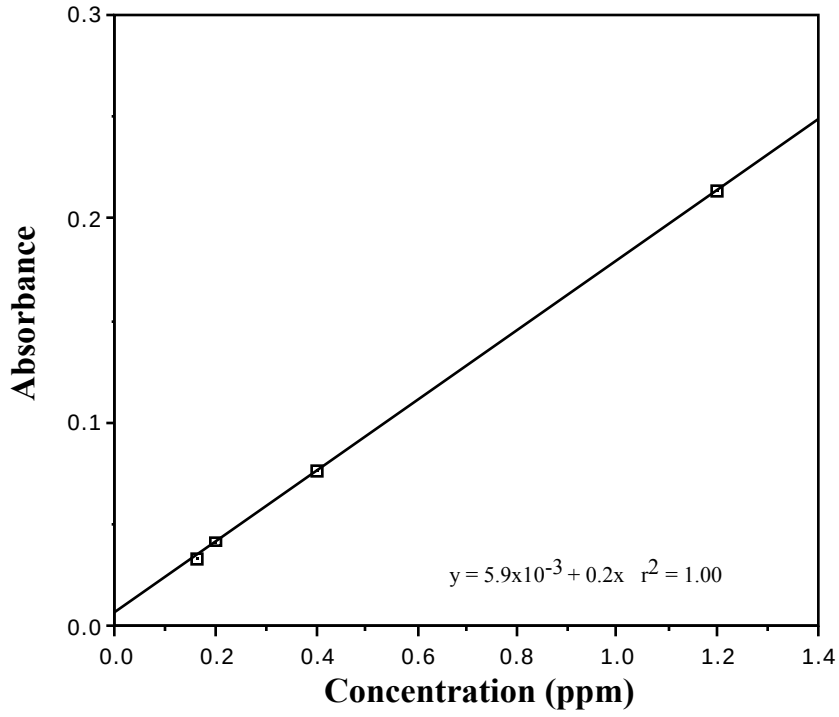

## Appendix 2: XRD patterns and XPS spectra

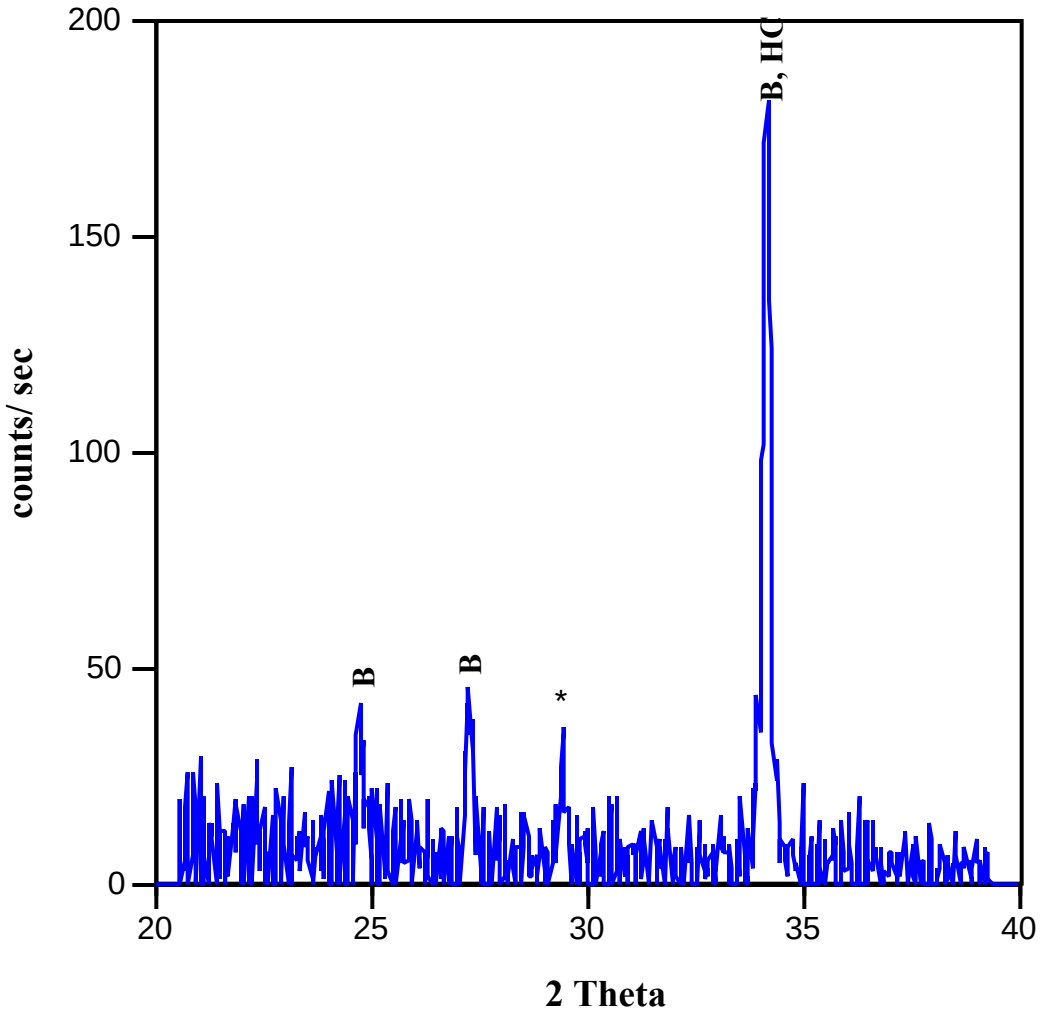


Figure B1.1: XRD pattern for suspended Pb precipitates in the borate buffered experiments. 'B' denotes $PbB_2O_4$, 'HC' denotes hydrocerrusite, and '*' denotes an unidentified peak. The experimental conditions were $\{Mn\}_i$ = 0 mg/L and $\{Pb\}_i$ = 3 mg/L and reaction time was 48 hours.

## Appendix 2: XRD patterns and XPS spectra

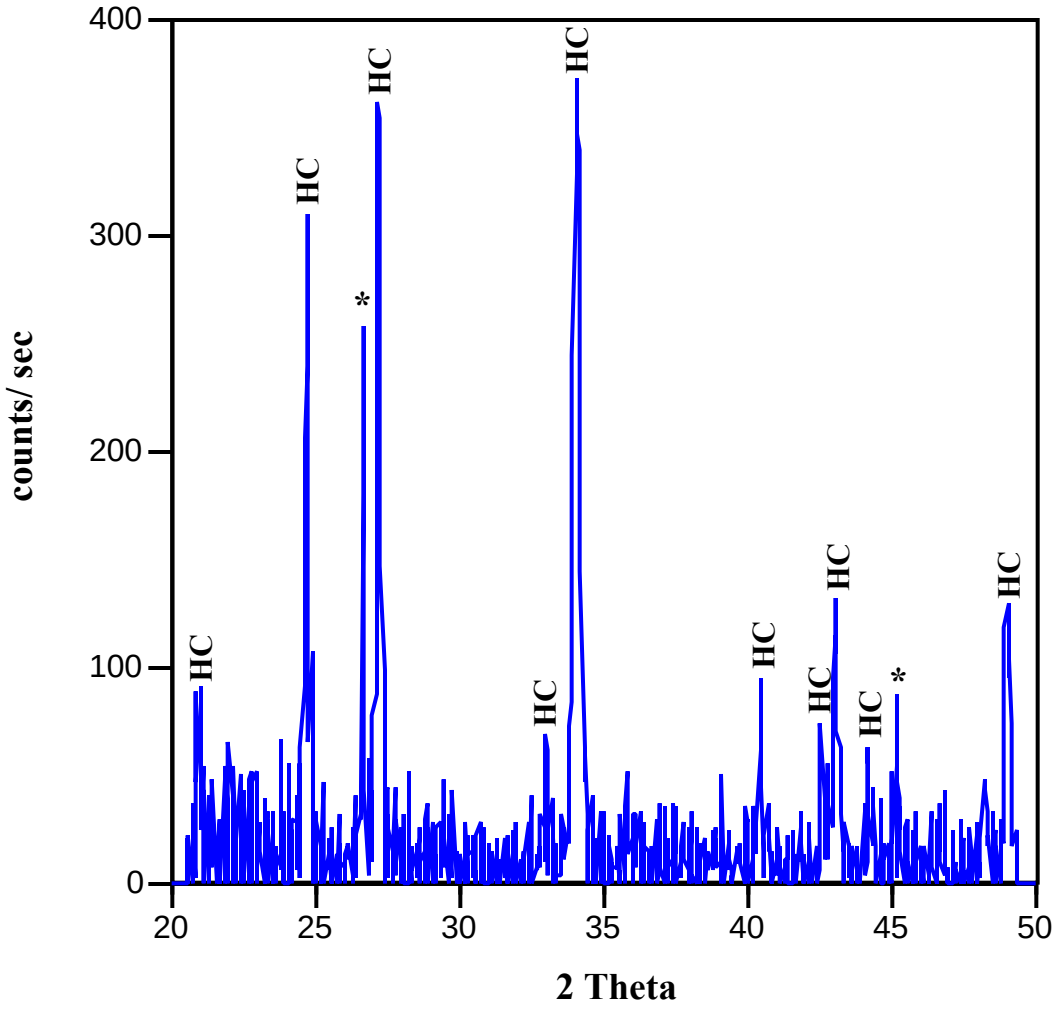


Figure B1.2: XRD pattern for suspended Pb precipitates in the bicarbonate buffered experiments. 'HC' denotes hydrocerrusite and '*' denotes an unidentified peak. The experimental conditions were $\{Mn\}_i$ = 0 mg/L and $\{Pb\}_i$ = 3 mg/L and reaction time was 48 hours.

**Appendix 2: XRD patterns and XPS spectra**

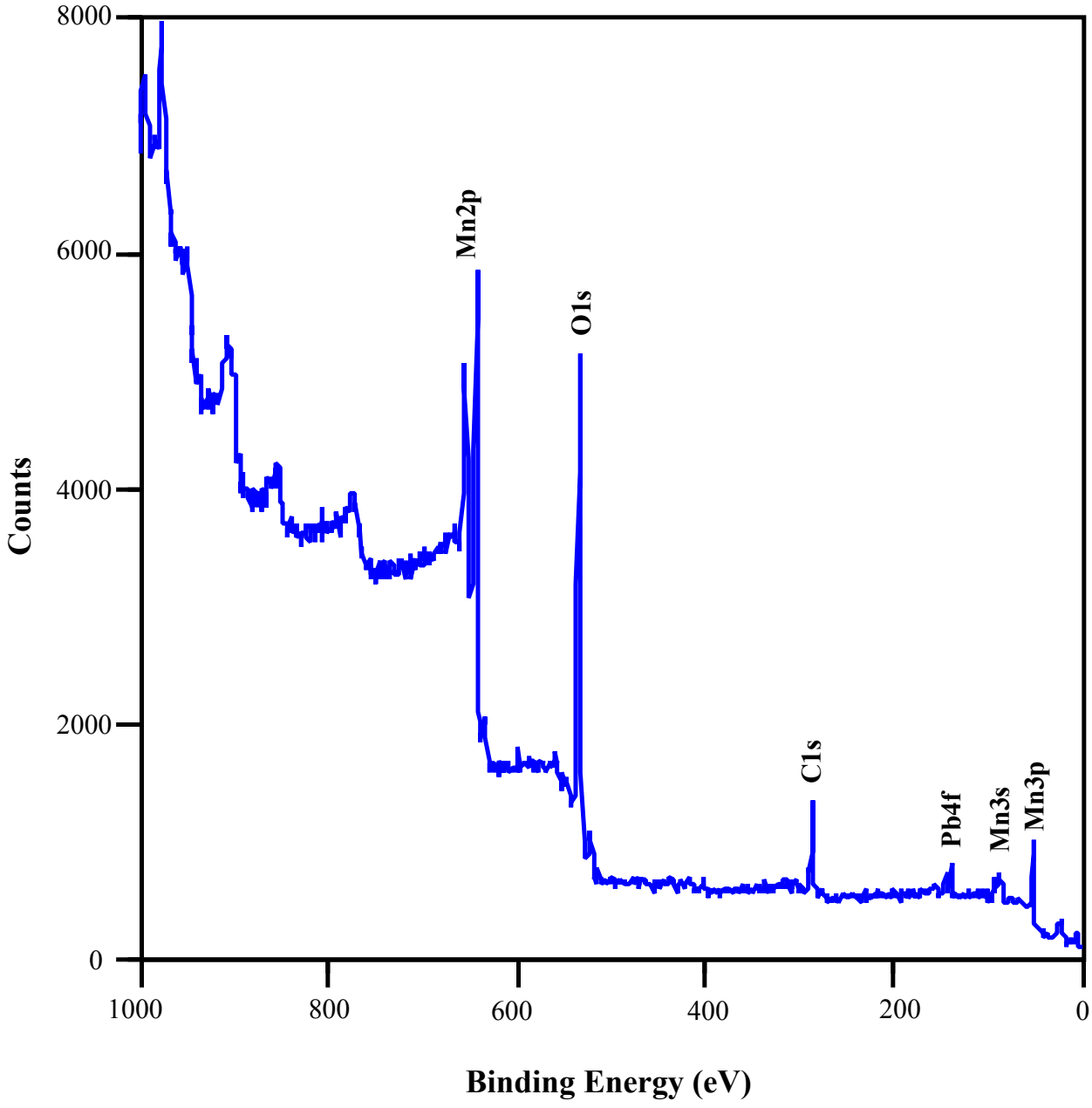


Figure C1.1: XPS spectra for quartz surfaces from sample brB7rha-2. Experimental conditions included $\{Mn\}_i$ = 100 mg/L, $\{Pb\}_i$ = 3 mg/L, reaction time of 60 days, and in the presence of the borate buffer.

## Appendix 2: XRD patterns and XPS spectra

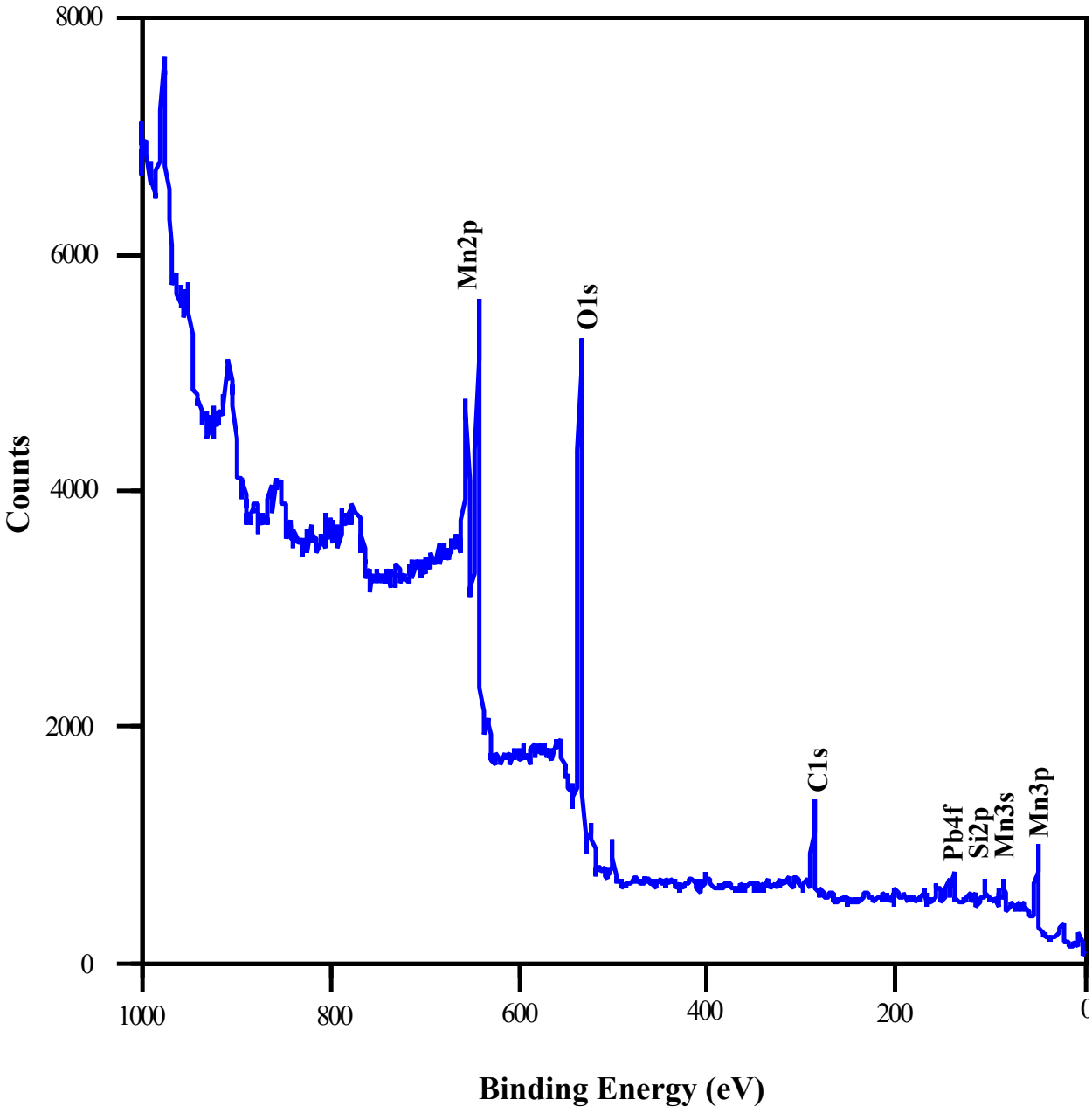


Figure C1.2: XPS spectra for quartz surfaces from sample brB8rha-1. Experimental conditions included $\{Mn\}_i$ = 100 mg/L, $\{Pb\}_i$ = 3 mg/L, reaction time of 48 hours, and in the presence of the borate buffer.

## Appendix 2: XRD patterns and XPS spectra

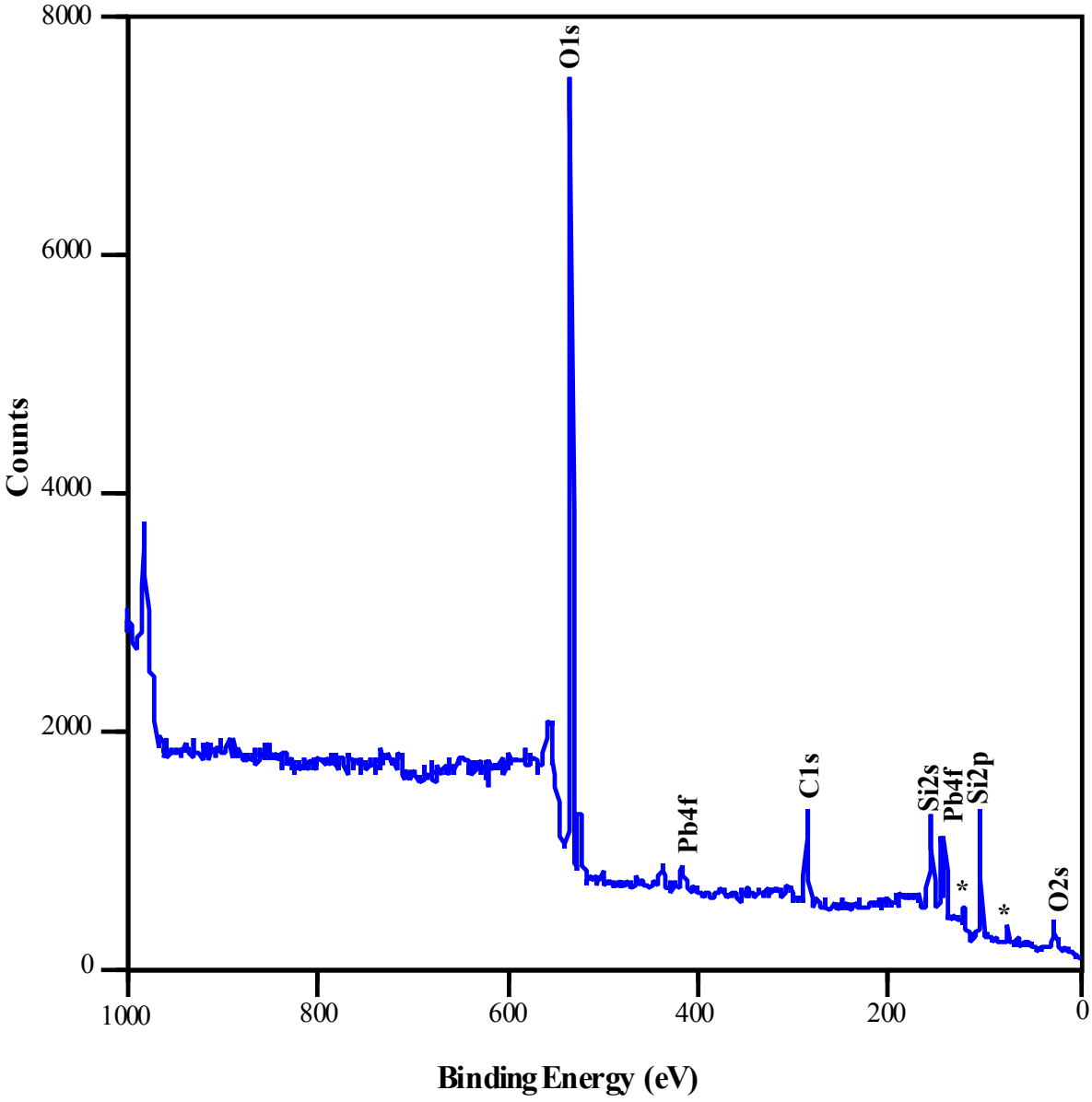


Figure C1.3: XPS spectra for quartz surfaces from sample brB8rha-6. Experimental conditions included $\{Mn\}_i = 0$ mg/L, $\{Pb\}_i = 3$ mg/L, reaction timeof 48 hours, and in the presence of the borate buffer. * denotes Al peaks from sample mount and/or clay minerals adhered to quartz surfaces.

**Appendix 2: XRD patterns and XPS spectra**

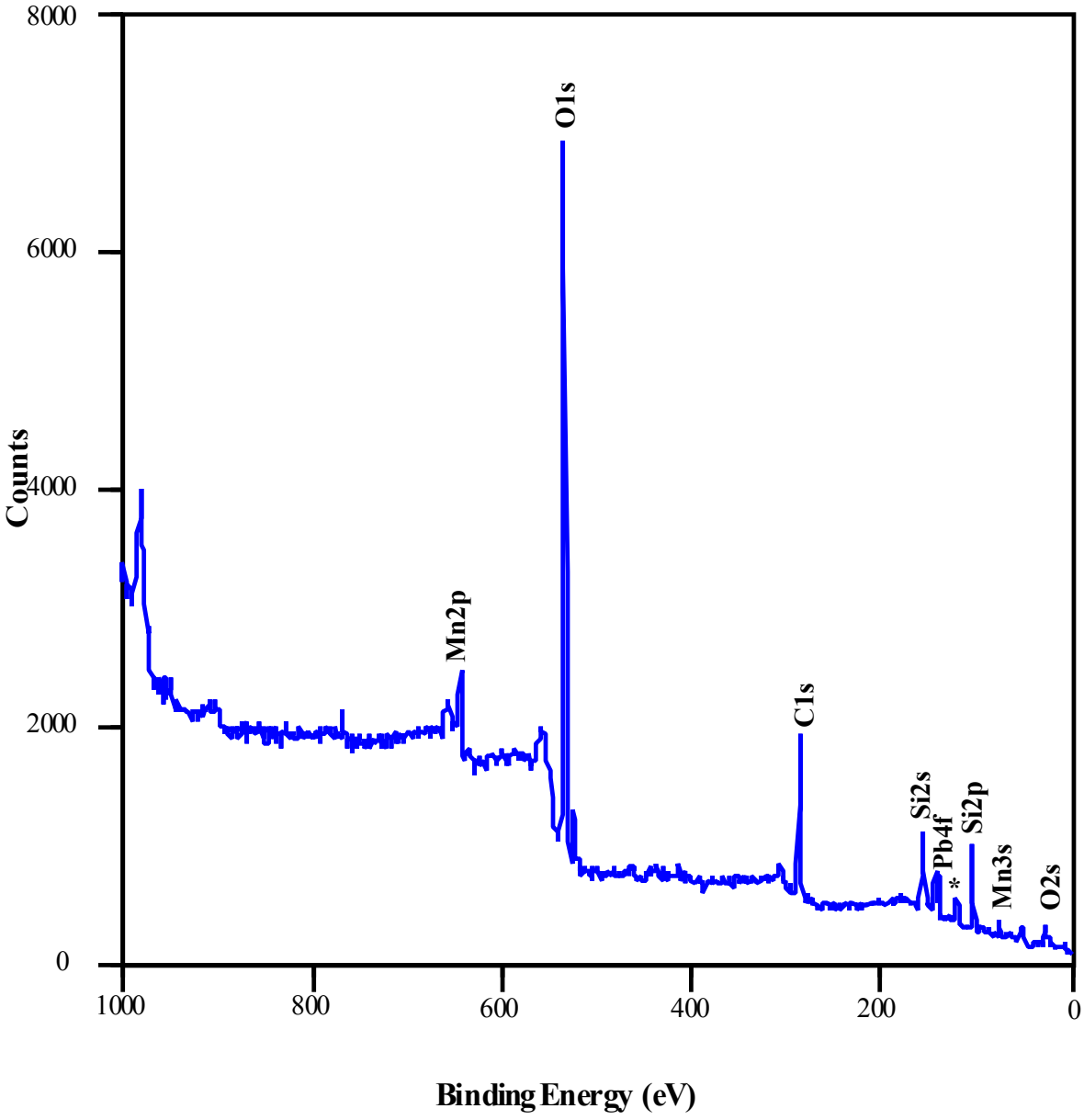


Figure C1.4: XPS spectra for quartz surfaces from sample brD5rha-1. Experimental conditions included $\{Mn\}_i$ = 100 mg/L, $\{Pb\}_i$ = 3 mg/L, reaction time of 48 hours, and in the presence of the bicarbonate buffer. * denotes Al peak from sample mount and/ or clay minerals adhered to the quartz surfaces.

**Appendix 2: XRD patterns and XPS spectra**

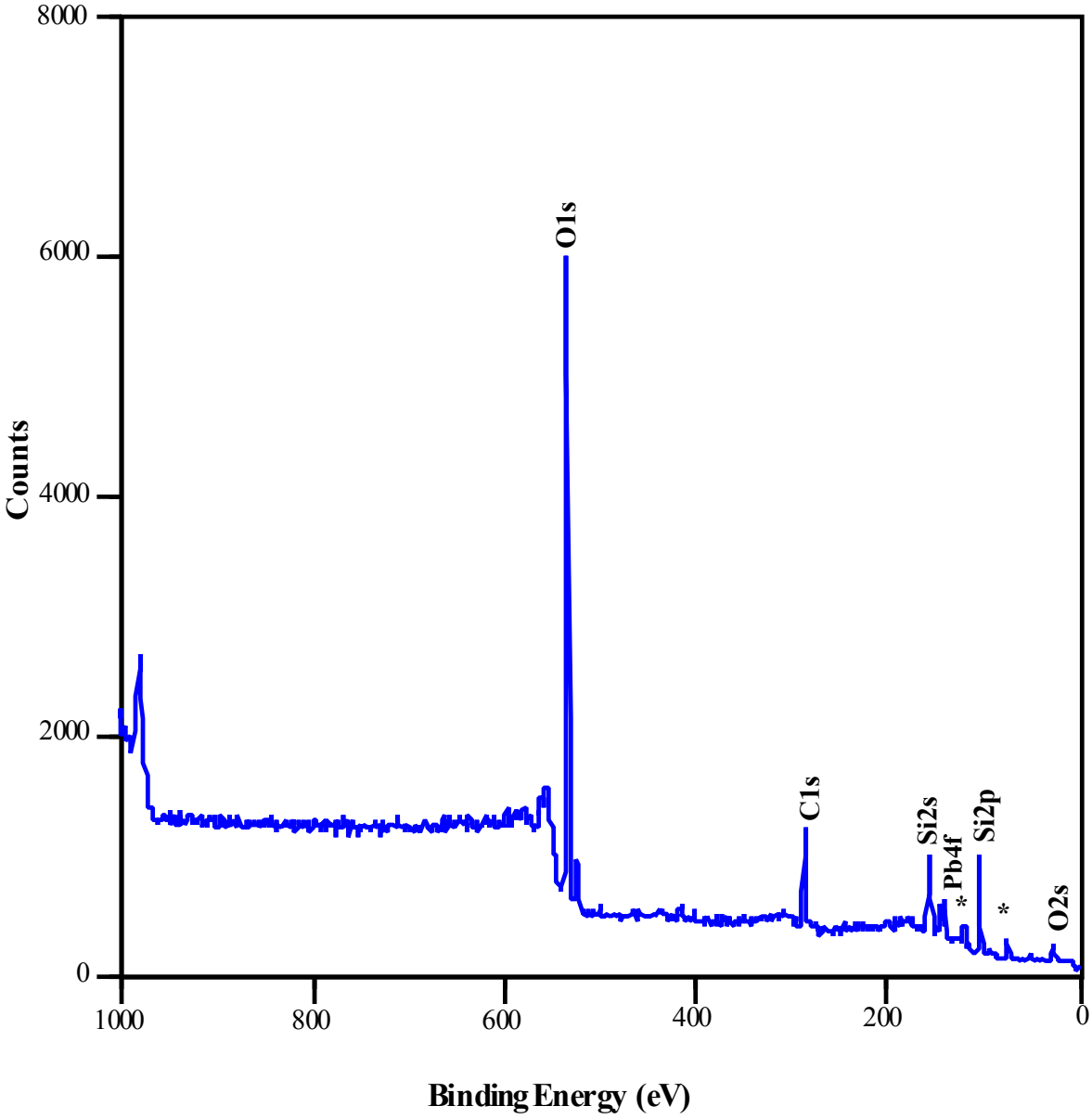


Figure C1.5: XPS spectra for quartz surfaces from sample brD5rha-6. Experimental conditions included $\{Mn\}_i$ = 0 mg/L, $\{Pb\}_i$ = 3 mg/L, reaction time of 48 hours, and in the presence of the bicarbonate buffer. * denotes Al peak from sample mount and/ or clay minerals adhered to the quartz surface.

## Appendix 3: Experimental Data

***A) Mn precipitated ({Mn}$_i$ - {Mn}$_{48hr}$ ) in borate buffered experiments:***

**{Pb}$_i$ = 3 mg/L:**

| {Mn}$_i$ | brB3rha | brB10rha | brB14rha | brB50rha | brB51rha | brB52rha |
|---|---|---|---|---|---|---|
| 100 | 12.94 | 32.96 | 12.94 | 21.52 | 21.52 | no data |
| 30 | 7.95 | 16.81 | 18.67 | 13.24 | 13.31 | 8.81 |
| 10 | 4.24 | 6.64 | 4.27 | 6.04 | 5.21 | 4.18 |
| 3 | <0.35 | 2.91 | <0.35 | 2.87 | 2.06 | 2.78 |
| 1 | <0.35 | 0.99 | <0.35 | 0.99 | 0.52 | 0.48 |
| 1 sigma error | 0.05 | 0.05 | 0.17 | 0.03 | 0.06 | 0.03 |

**{Pb}$_i$ = 1 mg/L:**

| {Mn}$_i$ | brB4rha | brB11rha | brB15rha |
|---|---|---|---|
| 100 | 27.24 | 19.23 | 30.38 |
| 30 | 21.03 | 11.45 | 14.96 |
| 10 | 4.98 | 4.21 | 7.61 |
| 3 | 1.62 | no data | 1.21 |
| 1 | 0.49 | 0.52 | 0.59 |
| 1 sigma error | 0.05 | 0.04 | 0.06 |

**{Pb}$_i$ = 0.3 mg/L:**

| {Mn}$_i$ | brB6rha | brB12rha | brB16rha |
|---|---|---|---|
| 100 | 32.39 | 25.81 | 30.97 |
| 30 | 13.10 | 8.66 | 6.81 |
| 10 | 3.70 | 5.55 | no data |
| 3 | 0.43 | 0.52 | no data |
| 1 | <0.35 | <0.35 | no data |
| 1 sigma error | 0.04 | 0.10 | 0.08 |

**{Pb}$_i$ = 0 mg/L:**

| {Mn}$_i$ | brB5rha | brB13rha | brB17rha |
|---|---|---|---|
| 100 | 24.66 | 22.95 | no data |
| 30 | 5.23 | 7.23 | 14.45 |
| 10 | <0.35 | <0.35 | 3.24 |
| 3 | <0.35 | <0.35 | <0.35 |
| 1 | <0.35 | <0.35 | <0.35 |
| 1 sigma error | 0.03 | 0.07 | 0.09 |

All values reported in mg/L. Average values reported in Table 4 of the Results section.

## Appendix 3: Experimental Data

***B) Mn precipitated ({Mn}i - {Mn}48hr) in bicarbonate system experiments:***

**$\{Pb\}_i$ = 3 mg/L:**

| $\{Mn\}_i$ | brD1rha | brD5rha | brD9rha | brD50rha | brD51rha | brD52rha |
|---|---|---|---|---|---|---|
| 100 | 25.24 | 16.66 | 15.51 | 24.95 | 19.52 | 14.94 |
| 30 | 4.37 | 7.73 | 4.16 | no data | 2.09 | 8.59 |
| 10 | 2.15 | 2.84 | 3.12 | 4.93 | 5.10 | 2.47 |
| 3 | <0.35 | 1.13 | 0.36 | 2.11 | 2.34 | 0.91 |
| 1 | <0.35 | 0.49 | <0.35 | 0.68 | 0.84 | 0.16 |
| 1 sigma error | 0.05 | 0.04 | 0.04 | 0.10 | 0.07 | 0.11 |

**$\{Pb\}_i$ = 1 mg/L:**

| $\{Mn\}_i$ | brD2rha | brD6rha | brD10rha |
|---|---|---|---|
| 100 | 17.23 | 10.08 | 12.37 |
| 30 | 6.45 | 18.20 | 6.73 |
| 10 | 2.47 | 2.12 | 2.55 |
| 3 | 0.65 | <0.35 | 0.79 |
| 1 | <0.35 | <0.35 | 0.38 |
| 1 sigma error | 0.03 | 0.04 | 0.08 |

**$\{Pb\}_i$ = 0.3 mg/L:**

| $\{Mn\}_i$ | brD3rha | brD7rha | brD11rha |
|---|---|---|---|
| 100 | 6.93 | 14.08 | 14.65 |
| 30 | 6.30 | 5.73 | 7.81 |
| 10 | 3.24 | 2.07 | 2.78 |
| 3 | 0.85 | 0.81 | 0.98 |
| 1 | <0.35 | <0.35 | <0.35 |
| 1 sigma error | 0.06 | 0.06 | 0.09 |

**$\{Pb\}_i$ = 0 mg/L:**

| $\{Mn\}_i$ | brD4rha | brD8rha | brD12rha |
|---|---|---|---|
| 100 | 9.22 | 3.50 | 8.94 |
| 30 | 8.88 | 5.30 | 2.66 |
| 10 | 1.84 | 0.95 | <0.35 |
| 3 | 0.45 | <0.35 | <0.35 |
| 1 | <0.35 | <0.35 | <0.35 |
| 1 sigma error | 0.03 | 0.02 | 0.03 |

All values reported in mg/L. Average values reported in Table 4 of the Results section.

## Appendix 3: Experimental Data

***C) Mn removal from solution as a function of time.***

**$\{Mn\}_t$ borate buffered experiments:**

| time (hours) | brB20rha | brB21rha | brB22rha |
|---|---|---|---|
| 3 | 10.00 | 10.00 | 10.00 |
| 6 | 10.00 | 10.00 | 10.00 |
| 12 | 9.42 | 7.93 | 6.79 |
| 24 | 7.87 | 6.79 | 5.30 |
| 36 | 7.28 | 4.85 | 3.96 |
| 48 | 6.08 | 5.10 | 3.30 |
| 1 sigma error | 0.07 | 0.11 | 0.08 |

**$\{Mn\}_t$ bicarbonate buffered experiments:**

| time (hours) | brD20rha | brD21rha | brD22rha |
|---|---|---|---|
| 3.00 | no data | no data | no data |
| 6 | 10.00 | 7.73 | 7.48 |
| 12 | 7.22 | 8.48 | 6.85 |
| 24 | 6.82 | 8.53 | 6.90 |
| 36 | 5.27 | 8.25 | 6.65 |
| 48 | 5.25 | 7.68 | 6.19 |
| 1 sigma error | 0.07 | 0.11 | 0.09 |

All values reported in mg/L.

***D) Nitric acid digestions: Amount of Mn associated with quartz surfaces.***

**$Q_{Mn}$ for borate buffered experiments:**

| $\{Mn\}_i$ | DibrB1rha | DibrB10rha | DibrB14rha | DibrB50rhaT | DibrB51rhaT | DibrB52rhaT |
|---|---|---|---|---|---|---|
| 100 | no data | no data | no data | 7.63 | 4.84 | 3.75 |
| 30 | no data | no data | no data | 3.97 | 4.04 | 2.21 |
| 10 | no data | no data | no data | 1.64 | <0.21 | 0.77 |
| 3 | no data | no data | no data | 1.82 | 1.04 | 0.26 |
| 1 | no data | no data | no data | 0.22 | 0.43 | 0.20 |
| 1 sigma error | | | | 0.15 | 0.03 | 0.01 |

## Appendix 3: Experimental Data

**$Q_{Mn}$ for bicarbonate buffered experiments:**

| $\{Mn\}_i$ | DibrD1rha | DibrD5rha | DibrD9rha | DibrD50rhaT | DibrD51rhaT | DibrD52rhaT |
|---|---|---|---|---|---|---|
| 100 | 0.94 | 0.51 | 1.98 | 1.88 | 2.24 | 1.07 |
| 30 | 0.37 | 0.21 | 1.23 | 1.88 | 0.92 | 1.26 |
| 10 | 0.35 | 0.31 | 0.63 | 0.84 | 0.97 | 1.00 |
| 3 | <0.21 | 0.21 | 0.20 | 1.22 | 0.81 | 1.51 |
| 1 | 0.38 | <0.21 | 0.32 | 0.78 | 0.47 | 0.52 |
| 1 sigma error | 0.10 | 0.09 | 0.10 | 0.10 | 0.07 | 0.05 |

**Amount of Mn associated with the quartz surface after acetic acid leaching:**

| | Borate buffered experiments: | | | Bicarbonate buffered experiments: | | |
|---|---|---|---|---|---|---|
| $\{Mn\}_i$ | DiHAcB50 | DiHAcB51 | DiHAcB52 | DiHAcD50 | DiHAcD51 | DiHAcD52 |
| 100 | 4.92 | 3.27 | 2.50 | 0.54 | 0.65 | 0.68 |
| 30 | 2.32 | 2.62 | 1.49 | 1.42 | 0.66 | 0.63 |
| 10 | 1.12 | <0.21 | 0.58 | 0.73 | 0.88 | 0.78 |
| 3 | 1.72 | 0.87 | <0.21 | 0.32 | 0.65 | 1.39 |
| 1 | <0.21 | 0.26 | <0.21 | 0.56 | 0.42 | 0.36 |
| 1 sigma error | 0.15 | 0.03 | 0.01 | 0.06 | 0.04 | 0.03 |

T denotes sum of Mn leached from surface (HAc leach) and Mn associated with surface (DiHAc): DiHAc data + HAc data. All values reported in $mg/m^2$. Average values are presented in Table 2 of the Results section.

***E) Acetic acid leach digestions: Amount of Mn extracted from quartz surfaces.***

**$E_{Mn}$ in borate buffered experiments:**

| $\{Mn\}_i$ | HAcB50rha | HAcB51rha | HAcB52rha |
|---|---|---|---|
| 100 | 2.72 | 1.57 | 1.24 |
| 30 | 1.66 | 1.42 | 0.71 |
| 10 | 0.52 | 0.22 | <0.21 |
| 3 | <0.21 | <0.21 | <0.21 |
| 1 | <0.21 | <0.21 | <0.21 |
| 1 sigma error | 0.05 | 0.05 | 0.09 |

## Appendix 3: Experimental Data

**$E_{Mn}$ in bicarbonate buffered experiments:**

| $\{Mn\}_i$ | HAcD50rha | HAcD51rha | HAcD52rha |
|---|---|---|---|
| 100 | 1.34 | 1.59 | 0.39 |
| 30 | 0.45 | 0.26 | 0.64 |
| 10 | <0.21 | <0.21 | 0.22 |
| 3 | 0.91 | <0.21 | <0.21 |
| 1 | 0.22 | <0.21 | <0.21 |
| 1 sigma error | 0.07 | 0.09 | 0.07 |

All values reported in mg/m$^2$. Average values are presented in Table 3 of the Results section

***F) Average percent Mn precipitated.***

**$\{Mn\}_i$ - $\{Mn\}_{48hr}$ (%):**

| $\{Mn\}_i$ (mg/L) | 3 ppm Initial $Pb^{2+}$ (%) | 1 ppm Initial $Pb^{2+}$ (%) | 0.3 ppm Initial $Pb^{2+}$ (%) | 0 ppm Initial $Pb^{2+}$ (%) |
|---|---|---|---|---|
| 100 | 20.4 (8.2) | 25.6 (5.8) | 29.7 (3.5) | 23.8 (1.2) |
| 30 | 43.8 (4.1) | 52.7 (4.9) | 31.7 (3.2) | 29.9 (4.9) |
| 10 | 50.9 (1.0) | 56.0 (1.8) | 46.3 (1.3) | 32.4 (0.1) |
| 3 | 75.7 (1.02) | 47.1 (0.3) | 15.9 (0.1) | |
| 1 | 74.6 (0.3) | 53.6 (0.1) | | |

**$\{Mn\}_i$ - $\{Mn\}_{48hr}$ (%):**

| $\{Mn\}_i$ (mg/L) | 3 ppm Initial $Pb^{2+}$ (%) | 1 ppm Initial $Pb^{2+}$ (%) | 0.3 ppm Initial $Pb^{2+}$ (%) | 0 ppm Initial $Pb^{2+}$ (%) |
|---|---|---|---|---|
| 100 | 19.5 (4.6) | 13.2 (3.7) | 11.9 (4.3) | 7.2 (3.2) |
| 30 | 18.0 (2.7) | 34.9 (6.7) | 22.0 (1.1) | 18.7 (3.1) |
| 10 | 34.3 (1.3) | 23.8 (0.2) | 27.0 (0.1) | 13.9 (0.6) |
| 3 | 45.6 (0.8) | 24.0 (0.1) | 29.3 (0.1) | 7.5 (0.1) |
| 1 | 49.3 (0.3) | 37.9 (0.1) | | |

1 sigma error reported in parentheses next to the value.

## Appendix 3: Experimental Data

***G) Pb associated with quartz surfaces [(QPb)t] as a function of time.***

| time (hours) | Borate: DibrB20rha | Bicarbonate: DibrD22rha |
|---|---|---|
| 6 | 0.00 | 0.00 |
| 12 | 0.24 | 0.17 |
| 24 | 0.49 | 0.24 |
| 36 | 0.59 | 0.20 |
| 48 | 0.59 | 0.31 |
| 1 sigma error | 0.05 | 0.09 |

All values in mg/m$^2$. The experimental conditions for these experiments were $\{Mn\}_i$ = 10 mg/L and $\{Pb\}_i$ = 3 mg/L.

***H) Nitric acid digestions: Amount of Pb associated with quartz surfaces.***

**$Q_{Pb}$ for borate buffered experiments:**

| $\{Mn\}_i$ | DibrB1rha | DibrB10rha | DibrB14rha | DibrB50rhaT | DibrB51rhaT | DibrB52rhaT |
|---|---|---|---|---|---|---|
| 100 | 0.87 | 0.52 | 0.44 | 0.28 | 0.52 | 0.24 |
| 30 | 0.74 | 0.52 | 0.44 | 0.52 | 0.38 | 0.35 |
| 10 | 1.05 | 0.46 | 0.57 | <0.12 | 0.38 | 0.28 |
| 3 | 0.79 | 0.52 | 0.66 | 0.49 | 0.45 | <0.12 |
| 1 | 0.44 | 0.31 | 0.35 | <0.12 | <0.12 | <0.12 |
| 0 | 0.28 | 0.26 | <0.12 | <0.12 | <0.12 | <0.12 |
| 1 sigma error | 0.10 | 0.11 | 0.05 | 0.04 | 0.07 | 0.05 |

**$Q_{Pb}$ for borate buffered experiments:**

| $\{Mn\}_i$ | DibrD1rha | DibrD5rha | DibrD9rha | DibrD50rhaT | DibrD51rhaT | DibrD52rhaT |
|---|---|---|---|---|---|---|
| 100 | 0.13 | 0.17 | 0.10 | <0.12 | 0.41 | 0.44 |
| 30 | 0.13 | <0.12 | 0.20 | 0.56 | 0.37 | 0.31 |
| 10 | 0.24 | 0.17 | 0.31 | 1.36 | 0.66 | 0.42 |
| 3 | 0.17 | 0.17 | 0.17 | 0.27 | 0.59 | 1.12 |
| 1 | <0.12 | 0.17 | <0.12 | 0.41 | <0.12 | 0.17 |
| 0 | <0.12 | <0.12 | <0.12 | <0.12 | 0.13 | 0.31 |
| 1 sigma error | 0.13 | 0.07 | 0.15 | 0.08 | 0.14 | 0.13 |

## Appendix 3: Experimental Data

**Amount of Pb associated with the quartz surface after acetic acid leaching:**

| | Borate buffered experiments: | | | Bicarbonate buffered experiments: | | |
|---|---|---|---|---|---|---|
| $\{Mn\}_i$ | DiHAcB50 | DiHAcB51 | DiHAcB52 | DiHAcD50 | DiHAcD51 | DiHAcD52 |
| 100 | <0.12 | 0.41 | 0.44 | <0.12 | 0.17 | 0.24 |
| 30 | 0.56 | 0.37 | 0.31 | 0.56 | 0.20 | 0.31 |
| 10 | 1.36 | 0.66 | 0.42 | 1.36 | 0.42 | 0.42 |
| 3 | 0.27 | 0.59 | 1.12 | 0.13 | 0.42 | 1.12 |
| 1 | 0.41 | <0.12 | 0.17 | 0.24 | <0.12 | <0.12 |
| 0 | <0.12 | 0.13 | 0.31 | <0.12 | <0.12 | <0.12 |
| 1 sigma error | 0.08 | 0.14 | 0.13 | 0.08 | 0.14 | 0.13 |

T denotes sum of Pb leached from surface (HAc leach) and Pb associated with surface (nitric acid digestion): DiHAc data + HAc data. All values reported in mg/m$^2$. Average values are presented in Table 2 of the Results section.

***I) Acetic acid leach digestions: Amount of Pb extracted from quartz surfaces.***

**$E_{Pb}$ for borate buffered experiments:**

| $\{Mn\}_i$ | HAcB50rha | HAcB51rha | HAcB52rha |
|---|---|---|---|
| 100 | <0.12 | <0.12 | <0.12 |
| 30 | <0.12 | <0.12 | <0.12 |
| 10 | <0.12 | <0.12 | <0.12 |
| 3 | <0.12 | <0.12 | <0.12 |
| 1 | <0.12 | <0.12 | <0.12 |
| 0 | <0.12 | <0.12 | <0.12 |
| 1 sigma error | 0.05 | 0.05 | 0.06 |

**$E_{Pb}$ for borate buffered experiments:**

| $\{Mn\}_i$ | HAcD50rha | HAcD51rha | HAcD52rha |
|---|---|---|---|
| 100 | <0.12 | 0.24 | 0.20 |
| 30 | <0.12 | 0.17 | <0.12 |
| 10 | <0.12 | 0.24 | <0.12 |
| 3 | 0.13 | 0.17 | <0.12 |
| 1 | 0.17 | <0.12 | 0.17 |
| 0 | <0.12 | 0.13 | 0.31 |
| 1 sigma error | 0.09 | 0.11 | 0.11 |

All values reported in mg/m$^2$. Average values are presented in Table 3 of the Results Section.

## Appendix 3: Experimental Data

***J) Amount of Mn precipitated ({Mn}i - {Mn}48hr) after 48 hours:***

| | **Borate** | **Bicarbonate** | **Borate** | **Bicarbonate** |
|---|---|---|---|---|
| $\{Mn\}_i$ | brN1rha | brN2rha | brN3rha | brN4rha |
| 100 | 18.09 | 7.79 | 19.23 | 2.93 |
| 30 | 6.09 | 4.09 | 8.81 | 5.30 |
| 10 | 0.66 | 2.01 | 4.58 | 1.35 |
| 3 | <0.35 | <0.35 | 1.79 | <0.35 |
| 1 | <0.35 | <0.35 | <0.35 | <0.35 |
| 1 sigma error | 0.23 | 0.24 | 0.01 | 0.09 |

These data are from experiments run without quarts grains. N1, N2 were run with $\{Pb\}_i = 0$ mg/L and N3, N4 were run with $\{Pb\}_i = 3$ mg/L. All values reported in mg/L

## Appendix 4: Mn precipitation rate calculations

To compare the rates in this study with those of Davies and Morgan (1989), a log $\{Mn\}_t$ versus time in minutes plot was prepared. The linear regression produced $1.24 \times 10^{-4}$ t - 3.72 for the borate buffered experiments and $5.98 \times 10^{-5}$ t - 3.78 for the bicarbonate buffered experiments. From Davies and Morgan (1989), the product of 2.303 and the derivative of the linear regression gives the rate constant: $k = 2.303 [d\{Mn\}_t /dt]$.

Borate buffered experiments: $k = 2.303 [1.24 \times 10^{-4}]$

$$k = 2.9 \times 10^{-4} \text{ min}^{-1}$$

Bicarbonate buffered experiments: $k = 2.303 [5.98 \times 10^{-5}]$

$$k = 1.4 \times 10^{-4} \text{ min}^{-1}$$

Then to recast the rate constant reported by Davies and Morgan (1989) to the conditions of this experiment, it was assumed that the surface area available for precipitation was the same in both studies. Differences in $P_{O2}$, $\{Mn\}_i$, and pH were also taken into account. Because the rate law proposed by Davies and Morgan (1989) is a linear relationship, their rate constant can be adjusted according to differences in these categories.

## Appendix 5: Coprecipitation of Cu with Mn oxyhydroxides

The following is the results of a series of experiments investigating Mn precipitation in the presence of Cu. These experiments were run to compare the effects of different metals in this system. All experiments were run under the same conditions and using the same methodology as the Mn-Pb experiments. Initial $Cu^{2+}$ was varied by half log units from 3 to 0 mg/L and added to solutions instead of $Pb^{2+}$. Experiments with Cu were only run in the presence of a borate buffer and quartz substrate. For a detailed description of the experimental and analytical methods refer to the Methods section and Appendix 1.

The tables and figures in this Appendix represent all the data collected in these experiments. No effort was made to interpret these data. Below is a brief summary of the observed results.

Very little Mn precipitation was visually observed associated with quartz surfaces or the walls of the batch reactors. Also, in all experiments where precipitation occurred, suspended precipitates were observed. In experiments with $\{Mn\}_i$ = 3 and 1 mg/L, no Mn precipitation occurred but a greenish-blue suspended precipitate did form. In the $\{Mn\}_i$ = 0 mg/L experiments, a blue suspended precipitate formed. XRD results identified the greenish-blue phase as copper borate hydroxide [$Cu_2(BO(OH)_2)(OH)_3$]. In experiments with $\{Mn\}_i$ = 10 mg/L, a green suspended precipitate was first observed. Over the duration of this experiment, the precipitate changed to a brown color. This precipitate was amorphous to X-rays.

Initial appearance of Mn precipitation was similar to the initial timing of first Mn precipitation in the Pb-borate system. Finally, Cu was determined to be present in a minority of final solutions using AA (detection = 0.1 mg/L), but, these data were not presented because they

were very erratic. The erratic nature can be attributed to the proximity of the data to the detection limit for Cu.

## Appendix 5: Coprecipitation of Cu with Mn oxyhydroxides

***Amount of Mn precipitated ($\{Mn\}_i$ - $\{Mn\}_{48hr}$) after 48 hours***

**3 mg/L initial Cu experiments:**

| $\{Mn\}_i$ | brC1rha | brC4rha | brC7rha | Avg. Mn pptd. | Stand. Dev. | %Mn pptd. |
|---|---|---|---|---|---|---|
| 100 | 20.95 | 20.66 | 22.09 | 21.23 | 0.76 | 21.23 |
| 30 | 3.16 | 5.80 | 3.30 | 4.09 | 1.49 | 13.63 |
| 10 | 5.06 | <0.35 | 2.32 | 3.69 | 1.94 | 36.92 |
| 3 | <0.35 | <0.35 | 0.28 | 0.28 | | 9.23 |
| 1 | <0.35 | <0.35 | <0.35 | | | |
| 1 sigma error | 0.05 | 0.05 | 0.03 | | | |

**1 mg/L initial Cu experiments:**

| $\{Mn\}_i$ | brC2rha | brC5rha | brC8rha | Avg. Mn pptd. | Stand. Dev. | %Mn pptd. |
|---|---|---|---|---|---|---|
| 100 | 18.37 | 36.96 | 30.96 | 28.76 | 9.49 | 28.76 |
| 30 | 8.95 | 5.52 | 17.39 | 10.62 | 6.11 | 35.39 |
| 10 | <0.35 | <0.35 | 0.18 | 0.18 | | 1.79 |
| 3 | <0.35 | <0.35 | <0.35 | | | |
| 1 | <0.35 | <0.35 | <0.35 | | | |
| 1 sigma error | 0.07 | 0.03 | 0.02 | | | |

**0.3 mg/L initial Cu experiments:**

| $\{Mn\}_i$ | brC3rha | brC6rha | brC9rha | Avg. Mn pptd. | Stand. Dev. | %Mn pptd. |
|---|---|---|---|---|---|---|
| 100 | 16.08 | 22.09 | no data | 19.09 | 4.25 | 19.09 |
| 30 | 4.95 | 6.16 | no data | 5.55 | 0.86 | 18.51 |
| 10 | 0.15 | <0.35 | no data | 0.15 | | 1.50 |
| 3 | <0.35 | <0.35 | no data | | | |
| 1 | <0.35 | <0.35 | no data | | | |
| 1 sigma error | 0.06 | 0.06 | | | | |

1 sigma error denotes the analysis error, pptd. denotes precipitated, avg. denotes average, and stand. dev. denotes standard deviation of the average. 0 mg/L Cu values presented in the proceeding figures are the same as the values used in the Pb borate experiments. All experiments were run for 48 hours, at 25°C, and pH 8.5 with the borate buffer. All values reported in mg/L, unless otherwise noted.

## Appendix 5: Coprecipitation of Cu with Mn oxyhydroxides

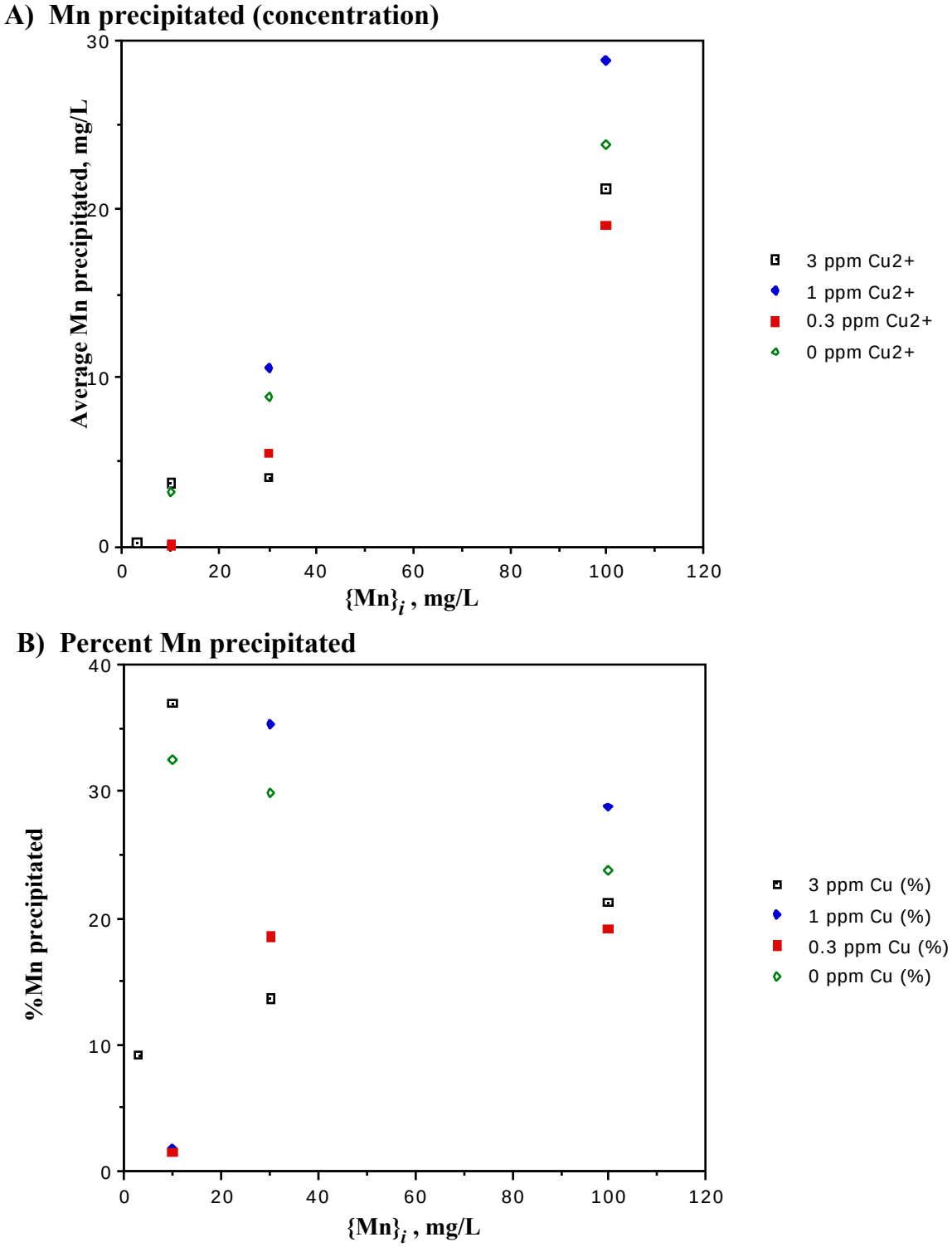


Figure 1: Total Mn precipitated from solution after 48 hours. Legend denotes initial concentration of Cu for a particular series of experiments. A) Concentration of Mn precipitated. B) Percent Mn precipitated.

## Appendix 5: Coprecipitation of Cu with Mn oxyhydroxides

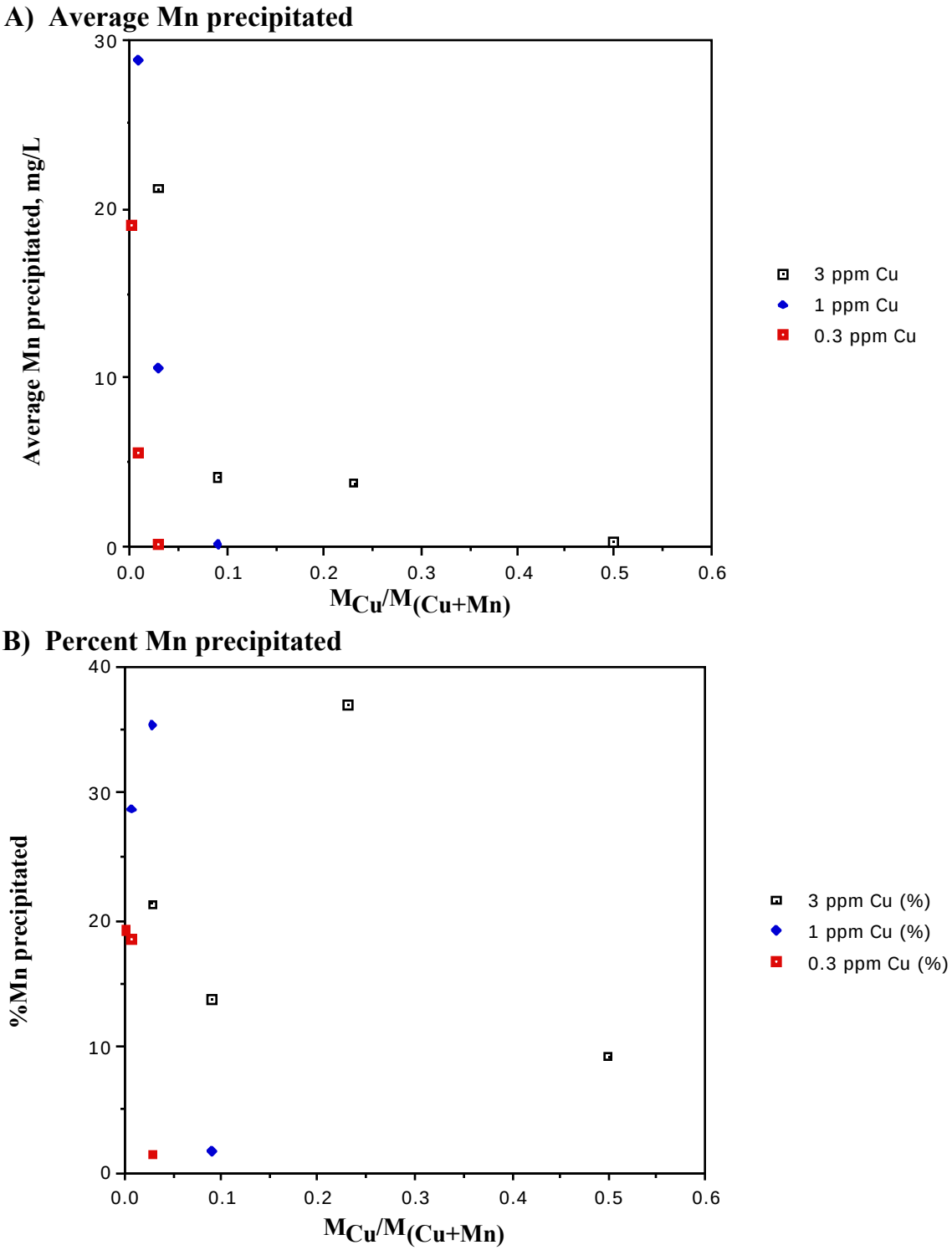


Figure 2: Total Mn precipitated as a function of initial Cu/ total metal ratio. Legend denotes initial Cu for a particular series of experiments. A) Average Mn precipitated. B) Percent Mn precipitated.

**Russell H. Abell**

Russell Abell was born on May 22, 1971 in Bangor, Maine. His family moved to Seekonk, Massachusetts in 1973 and still reside there today. Russell attended Seekonk High School and graduated in June, 1989. He then attended Amherst College in Amherst, Massachusetts graduating magna cum laude in May, 1993. After graduation he moved to Los Alamos, New Mexico to work as a graduate research assistant in the Earth and Geochemistry Group at Los Alamos National Laboratory. In October 1994, he started working as a field sampler with ICF Kaiser Engineers, Inc. of Los Alamos, New Mexico and moved to Santa Fe, New Mexico. In August, 1996, Russell moved to Blacksburg, Virginia to embark on a M.S. degree at Virginia Tech University. Russell graduated with his M.S. degree on May 9, 1998 and moved to Dallas, Texas to begin a position as an exploration geoscientist with Oryx Energy, Co.